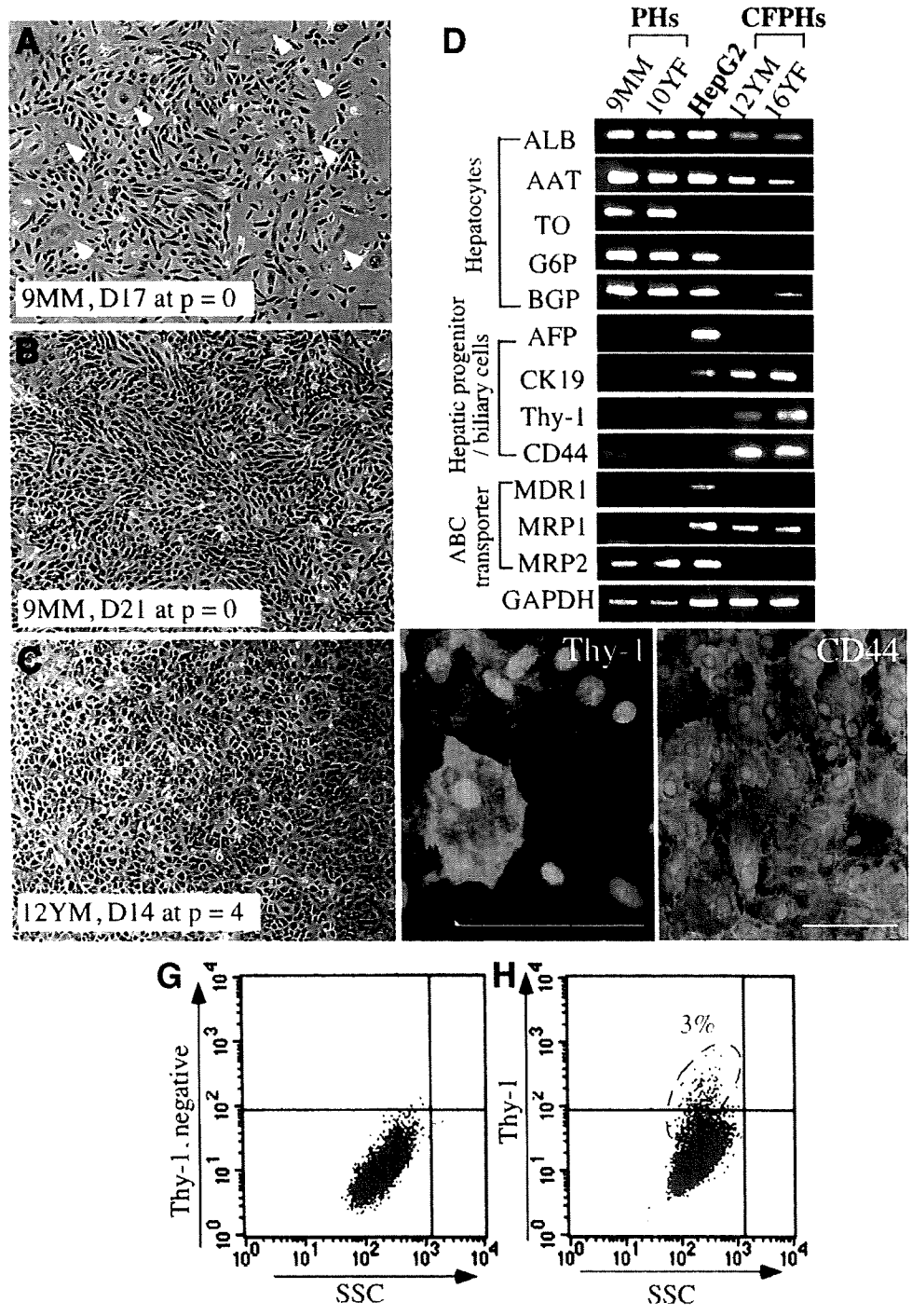

Fig. 1. CFPH growth and gene expression. (A-C) CFPH colony formation. We seeded 9MM PHs at 8 × 10^3 cells/cm^2 and cocultured with mitomycin C-treated Swiss 3T3 cells in *h*-hepatocyte clonal growth medium. A few CFPHs proliferated and formed colonies. CFPHs were cultured for (A) 17 and (B) 21 days. PHs were nonreplicative and were gradually expelled by replicative CFPHs. Arrowheads indicate the remaining flattened PHs, whose size increased. (C) Cryopreserved 12YM CFPHs (p = 3) were thawed and cultured in *h*-hepatocyte clonal growth medium with Swiss 3T3 cells for 14 days. (D) CFPH messenger RNA expression profiles. RNA was extracted from 9MM and 10YF PHs, HepG2 cells, and 12YM and 16YF CFPHs (p = 4). Semiquantitative RT-PCR was performed for ALB, AAT, TO, G6P, BGP, AFP, CK19, Thy-1, CD44, and the ABC transporters MDR1, MRP1, and MRP2. Glyceraldehyde-3-phosphate dehydrogenase (GAPDH) was used as an internal control. (E,F) Immunohistochemistry of Thy-1 and CD44. 12YM CFPHs (p = 4) were cultured for 14 days and stained for (E) Thy-1 and (F) CD44. The nuclei were stained with Hoechst 33258. Scale bar: 100 μm. (G,H) Flow cytometric analysis of CFPHs for Thy-1. Cells were suspended in Dulbecco's modified Eagle's medium containing 10% fetal bovine serum with (G) *m*-immunoglobulin G_1 as a negative control or (H) anti-*h*Thy-1 antibodies. Living cells were analyzed via fluorescence-activated cell sorting. A small fraction (3% in this case) of the CFPHs was Thy-1$^+$. Three independent analyses were performed with similar results.

given BrdU after 9 weeks. BrdU-positive CFPHs were observed at the edges of the colonies (Fig. 3E-G). Serial liver sections were prepared from CFPH-chimeric mice 9 to 10 weeks after transplantation for *h*ALB immuohistochemistry (Fig. 3H) and for *in situ* hybridization with an *h*-DNA probe (Fig. 3I). The regions identified as containing *h*-hepatocytes by the 2 methods were identical.

Comparison of Repopulation by CFPHs and PHs. PHs and CFPHs (p = 4) were prepared from the livers of 9MM and 12YM donors and transplanted into uPA/SCID mice, and the mice were killed 3 and 10 weeks posttransplantation. The transplanted cells were identified as *h*ALB-positive from histological sections. The number of PH- and CFPH-derived clusters was 125.0 ± 28.2 (n = 3) and 3.3 ± 7.5 (n = 7), respectively, per cross-section of the left lobe of the livers 3 weeks after transplantation, suggesting that the rate of engraftment of the CFPHs was much lower than that of the PHs.

The CFPHs were smaller in size compared with the PHs after 3 weeks (Fig. 4A-B). The cytoplasm of the

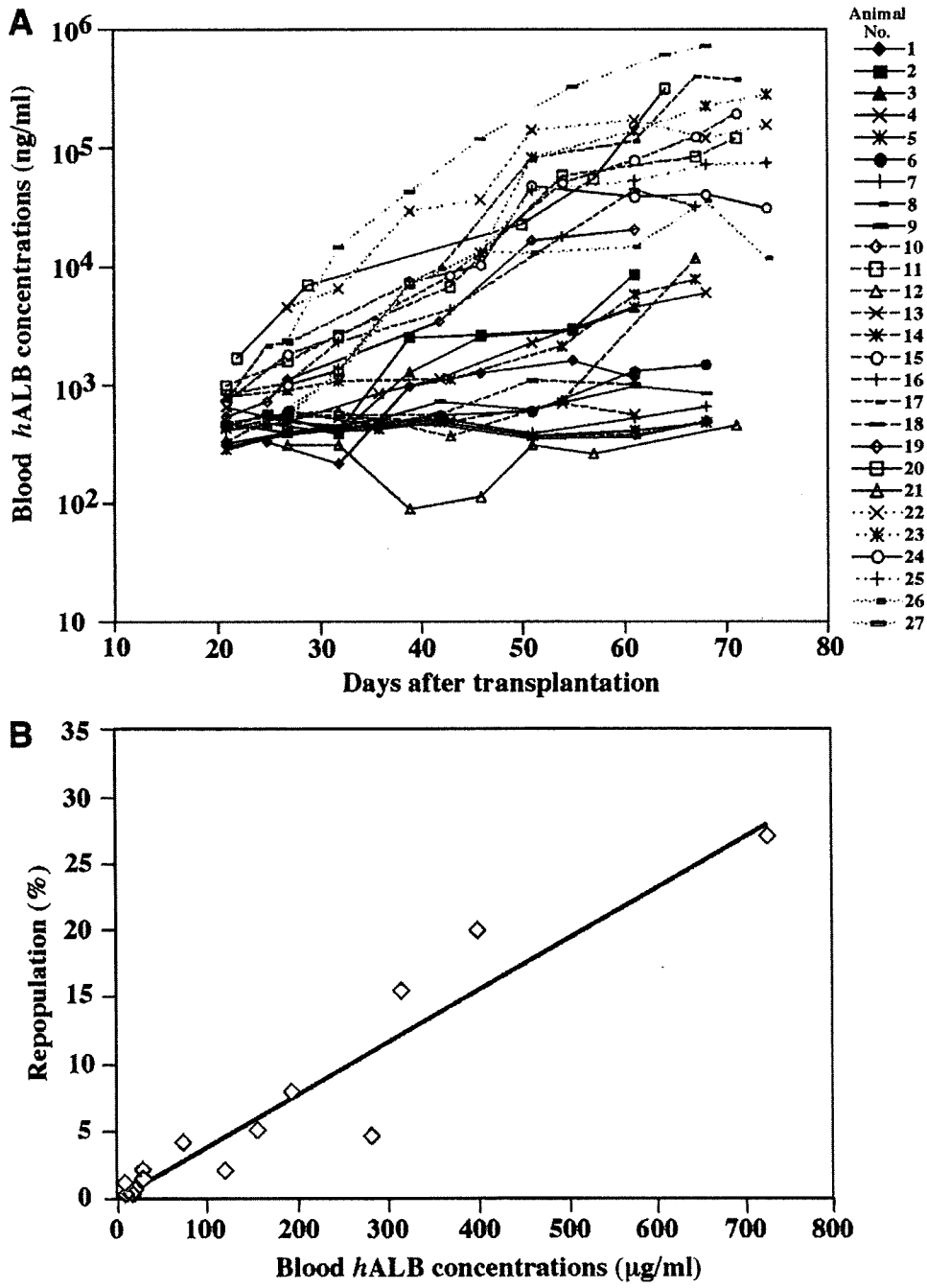

Fig. 2. Transplantation of CFPHs into uPA/SCID mice. The chimeric mice in this experiment are included in group D in Table 1. (A) We transplanted 12YM CFPHs (p = 4) into 27 mice and the serum level of *h*ALB was monitored individually. Ten hosts (animals 1, 5, 6, 7, 8, 9, 10, 13, 18, and 21) did not show significantly elevated *h*ALB levels during the experimental period. Four hosts (2, 3, 4, and 14) showed slight elevation. The *h*ALB concentration of 13 mice (11, 12, 15, 16, 17, 19, 20, 22, 23, 24, 25, 26, and 27) reached >10 μg/mL at 9 to 10 weeks after transplantation. (B) Correlation between the blood *h*ALB level and RI. Fourteen CFPH-chimeric mice (animals 2, 11, 12, 15, 16, 17, 19, 20, 22, 23, 24, 25, 26, and 27) were selected from the mice shown in panel A for RI determination. Their liver sections were immunostained for *h*ALB. RIs were determined for each animal and plotted against the *h*ALB concentration. The correlation coefficient (r^2) between the 2 parameters was 0.91.

former was less abundant and more strongly stained for *h*ALB than that of the latter. We observed *h*CD44 in the plasma membrane of the CFPH-derived cells (Fig. 4E), but not in that of the PH-derived cells (data not shown). At 10 weeks posttransplantation, the CFPHs had increased in size to match those of the PHs, whose sizes were unchanged (Fig. 4C-D), and *h*CD44 expression disappeared from the CFPH-derived cells (Fig. 4F). The diameter of each CFPH and PH was quantified as follows: 18.3 ± 5.1 μm (mean ± SD, n = 65) versus 25.8 ± 6.4 μm (n = 124) at 3 weeks and 27.0 ± 5.5 μm (n = 185) versus 25.8 ± 4.8 μm (n = 187) at 10 weeks. We found no significant differences in this parameter between the 12YM and 9MM samples. Thus, it appears that the CFPHs replicated without changing their original small size until 3 weeks posttransplantation, when they became larger.

Liver sections from the chimeric mice were stained with hematoxylin-eosin to compare the morphological features of PHs and CFPHs at 10 weeks. The repopulated CFPHs (Fig. 4G) showed no significant difference in morphology compared with the repopulated PHs (Fig. 4H). As reported previously,[5,6] the PHs in the chimeric livers were enlarged and had less eosinophilic cytoplasm

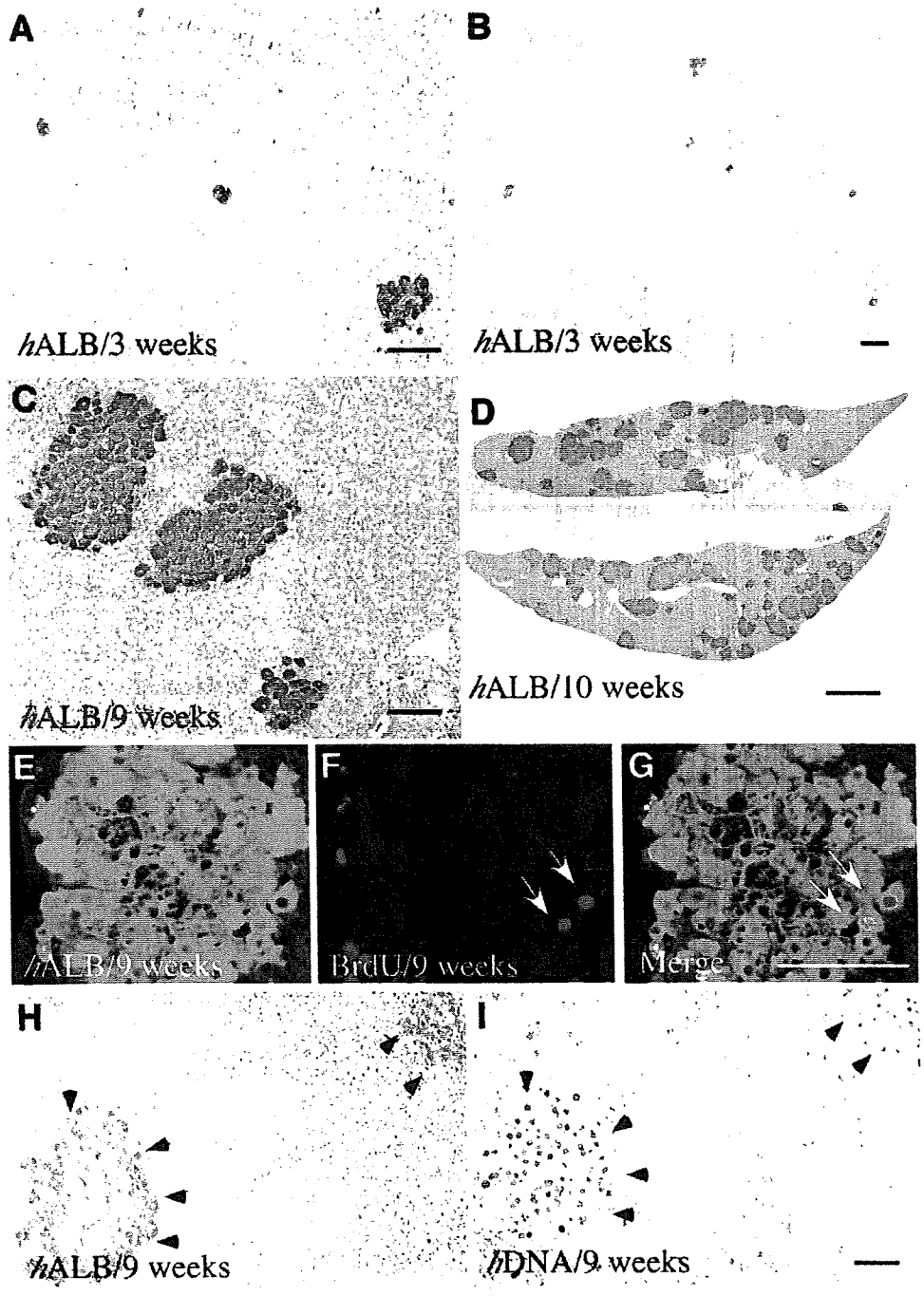

Fig. 3. Engraftment and repopulation of CFPHs in chimeric mouse liver. The chimeric mice in this experiment are included in groups A and D in Table 1. We performed *h*ALB immunohistochemistry using liver sections from CFPH-chimeric mice (A,B) 3, (C) 9, and (D) 10 weeks after transplantation. (A,B) Small clusters composed of 1-25 cells were scattered throughout the liver at 3 weeks in 3 of 9 mice. (C,D) The clusters became larger at 9 to 10 weeks. The liver sections in panel C were prepared from animal 2 in Fig. 2A (RI = 1.1%). The liver sections in panel D were prepared from animals 17 (RI = 20.0%; upper section) and 27 (RI = 27.0%; lower section). Three mice were randomly selected for the BrdU incorporation experiments (animals 2, 19, and 20 in Fig. 2A). They were given BrdU 1 hour before death at 9 weeks posttransplantation. Serial liver sections were subjected to (E) *h*ALB- and (F) BrdU immunohistochemical staining. The image in panel G is panel E and panel F merged. Similar results were obtained from these experiments, and the result from animal 19 (RI = 0.6%) is shown in panels E-G. Serial liver sections were prepared from CFPH-chimeric mice (animals 2, 15, and 17 in Fig. 2A) 9 to 10 weeks after transplantation for *h*ALB immunohistochemistry (H) and for *in situ* hybridization with an *h*-genomic probe (I). Similar results were obtained from the 3 mice. The results shown in panels H and I were obtained from animal 2 (positive cells are indicated by arrowheads). Scale bars in panels A-C, G, and I: 100 μm. Scale bar in panel D: 1 cm.

than the PHs in *h*-livers. The livers of the mice that had low *h*ALB levels at 10 weeks posttransplantation were mostly occupied by red nodules, which have been reported to be formed by the transgene-deleted hepatocytes of the host.[20]

Gene and Protein Expression Profiles of CFPHs in Chimeric Mice Compared with Those of PHs. Three 12YM CFPH-chimeric mice (11, 15, and 17) were randomly selected from the mice in Fig. 2A and killed 10 weeks after transplantation. RNA was extracted from each liver to generate gene expression profiles via RT-PCR. RT-PCR was also performed on 2 12YM PH-chimeric mice that were included in a previous study.[5] The CFPH livers expressed *h*ALB, *h*AAT, *h*TO, *h*G6P, and *h*MRP2, but not *h*CK19, *h*Thy-1, or *h*MRP1, just as in the PH-livers (Fig. 5). Previously, we showed that the PHs in chimeric mice expressed various *h*-cytochrome P450 (*h*CYP) subtypes in a manner similar to the donor liver.[5] In this study, we found that the expression of *h*CYPs 1A2, 2C8, 2C9, 2D6, and 2E1, but not 3A4, in the CFPH-chimeric mice was similar to that in the PH-chimeric mice (data not shown). Expression of *h*CYP3A4 was very

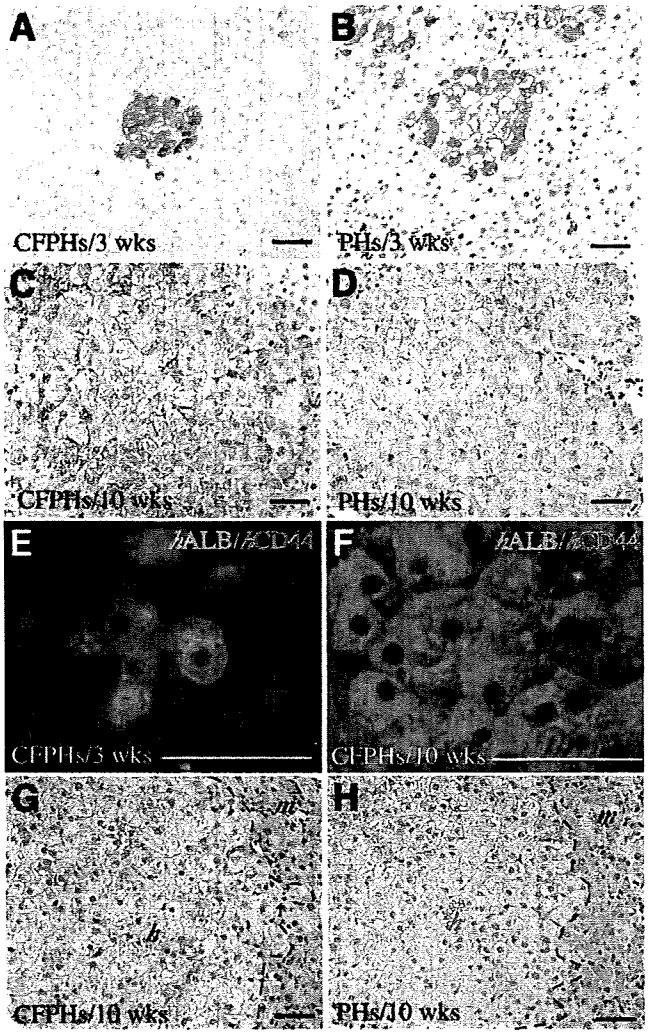

Fig. 4. Immunohistochemical staining for CFPHs and PHs in chimeric mice. Immunohistological analysis with antibodies against (A-D) *h*ALB and (E-F) *h*CD44. We produced 3 12YM CFPH-chimeric mice and 4 9MM CFPH-chimeric mice [(A) and (E), included in groups A and B in Table 1] and 3 9MM PH-chimeric mice [(B), group C], which were killed at 3 weeks posttransplantation. At 10 weeks posttransplantation, 3 12YM CFPH-chimeric mice that were randomly selected from the mice shown in Fig. 2A (15, 16, and 17) were killed [(C) and (F), group D), as were 9MM and 12YM PH-chimeric mice, 2 mice each [(D), groups E and F]. (A-D) Representative images of liver sections prepared from the animals and stained with anti-*h*ALB antibodies. The diameters of the *h*ALB-positive cells were measured in 10-15 randomly selected fields. (E,F) Double-fluorescence immunostaining. Green and red stains depict *h*ALB and *h*CD44, respectively. (G,H) Hematoxylin-eosin staining. (G) Eight CFPH mice were randomly selected from the mice shown in Fig. 2A and killed at 10 weeks posttransplantation. Their liver tissues were then subjected to hematoxylin-eosin staining. (H) Three 12YM PH-chimeric mice were killed at 10 weeks posttransplantation for hematoxylin-eosin staining as above. Similar results were obtained for the 8 CFPH-chimeric mice and 3 PH-chimeric mice. (E-F) Sections from (E) a CFPH-chimeric mouse (RI = 20.0%) and (F) a PH-chimeric mouse (RI = 57%). *h*, *h*-hepatocyte region; *m*, *m*-hepatocyte region. Dashed lines show the boundary between the 2 regions. Scale bars: 50 μm.

low (less than one-fifth) in CFPHs compared with that in PHs.

Protein expression was investigated immunohistochemically for the CFPH-chimeric livers at 3, 9, and 10 weeks posttransplantation. All of the examined CFPHs were Thy-1–negative, CK7-negative, CK19-negative, and AFP-negative (data not shown). The *h*ALB-positive cells were coincident with the *h*CK18-positive cells at both 3 (data not shown) and 9 weeks posttransplantation (Fig. 6A-C). MRP2-positive signals were present on the bile canalicular membranes of the transplanted CFPHs at 10 weeks (Fig. 6D-F). CYP3A4-expressing CFPHs were localized in the pericentral zone (Fig. 6G-I) as reported previously,[21] but their distributions were unique. Although some of the CFPHs were positive for CYP3A4, approximately 70% of them were negative. In contrast, all of the CFPHs in the pericentral zone strongly expressed CYP1A2 (Fig. 6J-L), which is known to be expressed in postnatal liver.[22] The CFPHs in the chimeric mice were strongly PAS-positive (Fig. 6N), whereas the *in vitro* CFPHs were faintly PAS-positive (data not shown). From

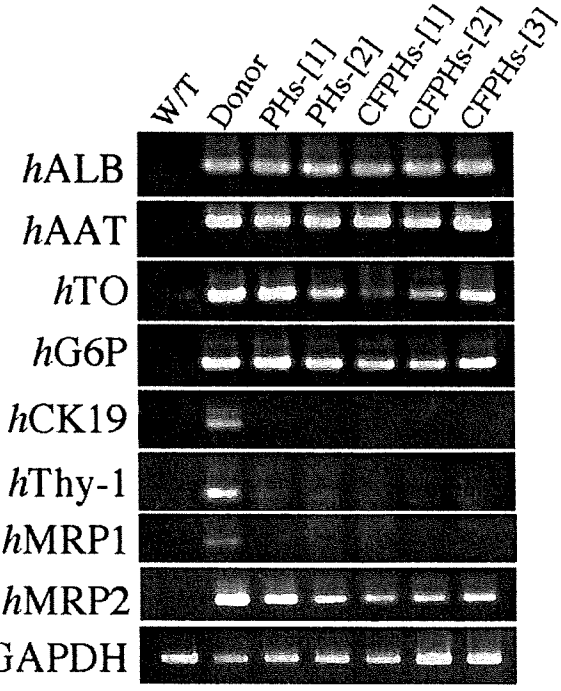

Fig. 5. Gene expression profiles of CFPHs in chimeric mice. Two uPA/SCID mice were transplanted with 12YM PHs ([1] and [2]); 3 uPA/SCID mice were transplanted with 12YM CFPHs ([1], [2], and [3]). The chimeric mice in this experiment are included in groups D and F in Table 1. After 10 weeks, the livers were removed for RT-PCR analysis. At the time of death, the PH-[1]-, PH-[2]-, CFPH-[1]-, CFPH-[2]-, and CFPH-[3]-chimeric mice had RIs of 41.0%, 57.0%, 2.1%, 7.9%, and 20.0%, respectively. The analysis was repeated using liver tissues from donor and uPA/SCID mice without transplantation (W/T). Glyceraldehyde-3-phosphate dehydrogenase (GAPDH) amplification was used as an internal control.

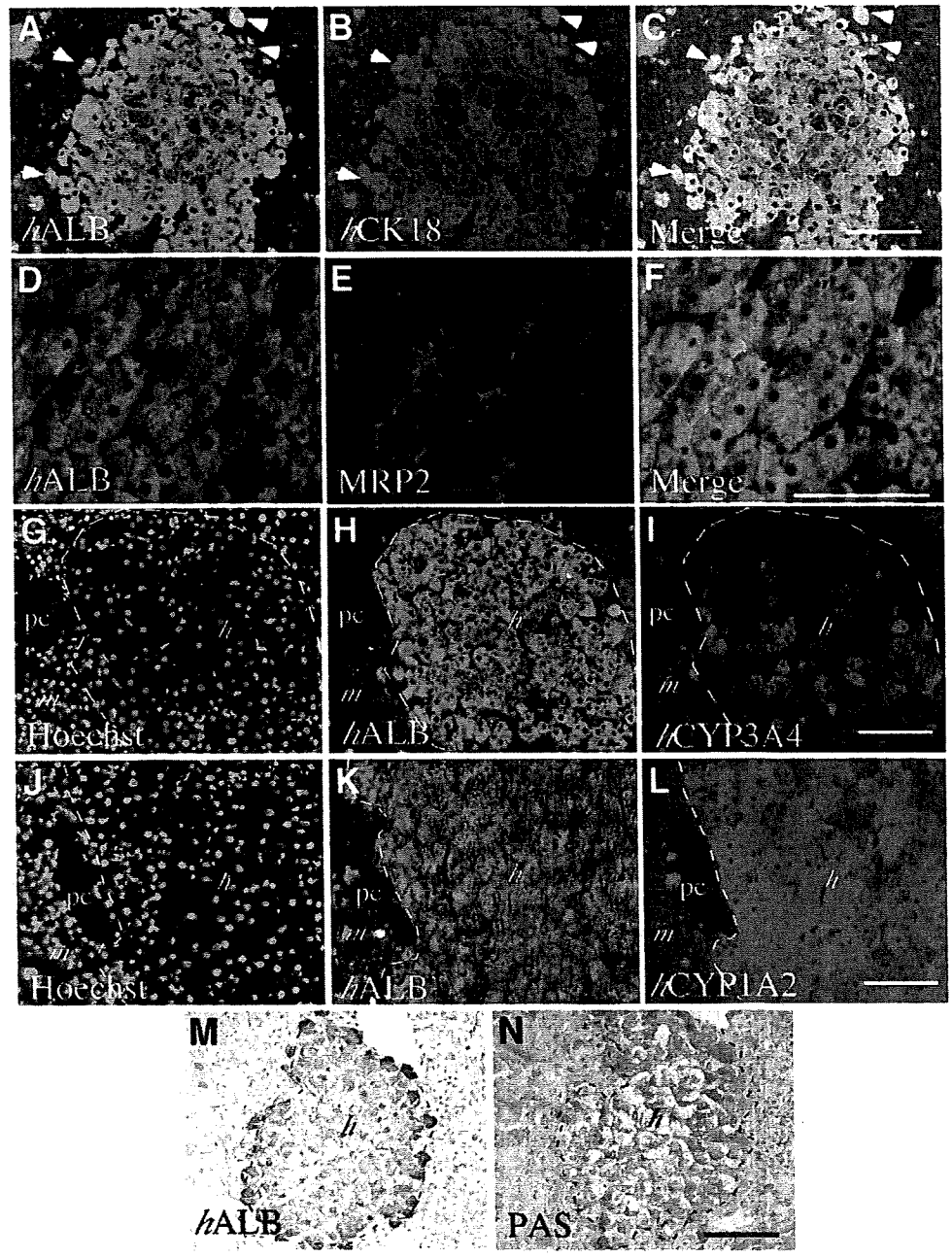

Fig. 6. Protein expression profiles of the CFPHs in chimeric livers. Mice were transplanted with 12YM CFPHs, and their livers were removed 9 to 10 weeks after transplantation for immunohistochemical analysis of (A,D,H,K) *h*ALB, (B) *h*CK18, (E) MRP2, (I) CYP3A4, and (L) CYP1A2. The chimeric mice in this experiment are included in group D in Table 1. Representative images are shown. (A-F) Double-fluorescence immunostaining. (A,D) *h*ALB is stained green. (B) *h*CK18 and (E) *h*MRP2 are stained red. Panels A and B were merged to create panel C; panels D and E were merged to create panel F. The arrowheads in panels A-C show macrophages engulfing such wastes as lipids. Serial sections of liver tissues subjected to 2 series of immunohistochemical examinations, one for (G-I) *h*CYP3A4 and the other for (J-L) *h*CYP1A2. The sections were stained with (G,J) Hoechst 33258, and for (H,K) *h*ALB, (I) *h*CYP3A4, and (L) *h*CYP1A2. Serial sections of liver tissues at 9 weeks posttransplantation were subjected to *h*ALB-immunostaining (M) and PAS staining (N). The positive cells appear brown in (M) and red in (N). *h*, *h*-hepatocyte region; *m*, *m*-hepatocyte region; pc, pericentral zone. Dashed lines show the boundary between the *h*-hepatocyte and *m*-hepatocyte regions. Scale bars: 100 μm.

these results, we conclude that the transplanted CFPHs differentiated into functionally mature hepatocytes. No *h*-cell tumors were formed during any of our experiments in the uPA/SCID mice.

Infection of CFPH-Chimeric Mice with HBV. To further examine whether CFPHs had exhibited normal differentiated phenotypes in chimeric mice, we tested their susceptibility to HBV infection. Four CFPH-chimeric mice with various serum *h*ALB levels (0.2, 1.6, 7.3, and 222.0 μg/mL) were inoculated with 100 μL of HBV-positive *h*-serum at 9-12 weeks posttransplantation. The animals were then tested every 2 weeks for HBV viremia and serum *h*ALB levels (Fig. 7A). The amount of HBV DNA in the animals increased between 2 and 8 weeks after inoculation, and all 4 mice developed measurable viremia within 8 weeks. However, a correlation was observed between the HBV DNA and/or HBsAg level and the *h*ALB level: the former appeared to be high when the latter was high (Fig. 7A). HBsAg was detectable in the serum of the chimeric mice when they showed elevated virus titers: the HBsAg levels of chimeric mice with HBV DNA levels of 2×10^3, 5.2×10^5, 5.9×10^7, and 7.7×10^8 copies/mL 8 weeks after inoculation were <0.05, <0.05, 3.2, and 124.0 IU/mL, respectively. HBV was infectious to CFPH-chimeric mice with very low levels of *h*ALB ($<10^4$ ng/mL), and all mice showed quantitatively

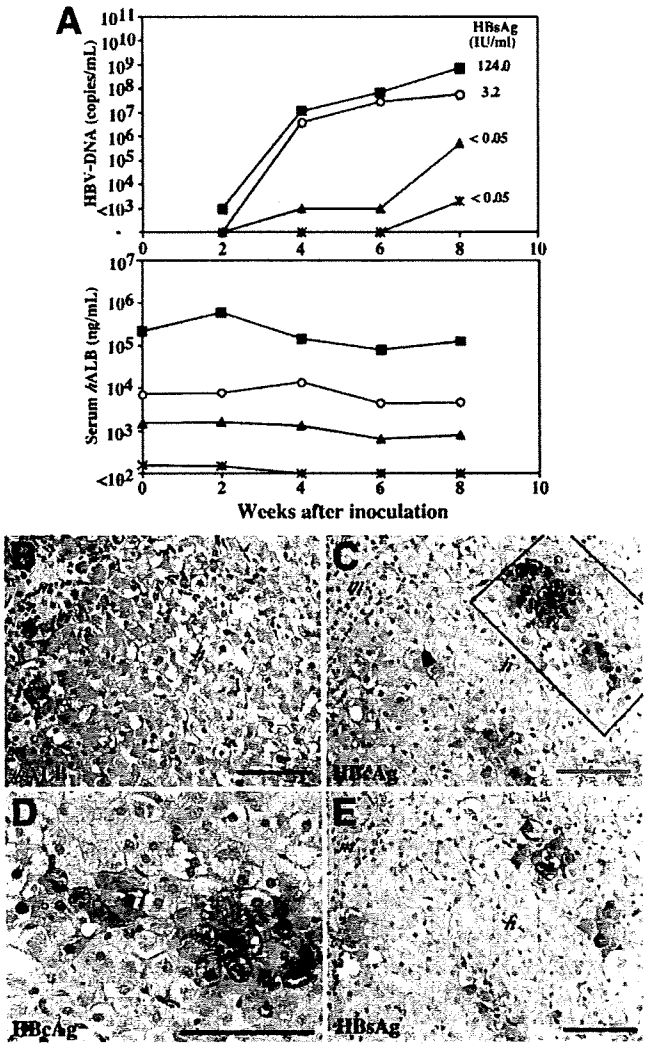

Fig. 7. Susceptibility of chimeric mice to infection with HBV. The chimeric mice in this experiment are included in group G in Table 1. uPA/SCID mice were transplanted with 12YM CFPH (p = 4). (A) The serum *h*ALB concentration of each mouse was determined 9-12 weeks posttransplantation just before the mouse was intravenously injected with 100 μL of HBV-positive *h*-serum (0.2 μg/mL at 12 weeks, 1.6 μg/mL at 10 weeks, 7.3 μg/mL at 11 weeks, and 222.0 μg/mL at 9 weeks). The animals were examined every 2 weeks for HBV viremia and serum *h*ALB level. The upper and lower graphs show the HBV DNA levels (copies/mL) and serum *h*ALB concentrations (ng/mL), respectively. The amount of HBV DNA ($<10^3$ copies/mL) was semiquantitatively measured via nested PCR. The values in the upper graph represent the HBsAg levels at 8 weeks. (B-E) Immunohistochemical analysis of chimeric livers infected with HBV. Serial sections of liver tissues at 8 weeks after inoculation were stained for (B) *h*ALB, (C,D) hepatitis B core antigen, and (E) HBsAg. The region enclosed by a square in panel C is magnified in panel D. Scale bars: 100 μm.

measurable viremia ($>10^3$ copies/mL) up to 8 weeks after inoculation. In contrast, most PH-chimeric mice with $<10^4$ ng/mL *h*ALB did not show quantitatively measurable levels of viremia up to 12 weeks after inoculation (data not shown) as reported previously.[8] In this study, we confirmed that CFPHs were not susceptible to infection with HBV prior to transplantation. The presence of hepatitis B core antigen and HBsAg in the CFPHs from HBV-infected chimeric livers was examined immunohistochemically (Fig. 7C,E). CFPHs were positive for both antigens that were sporadically distributed in the same regions among the CFPH colonies. Hepatitis B core antigen–positive cells accounted for 18.7 ± 8.3% of the total number of CFPHs (n = 3; total cell count = 1,215) (Fig. 7C), and both the nucleus and cytoplasm of the cells showed signals (Fig. 7D).

Discussion

This study supports our previous conclusion that CFPHs are *h*-hepatic progenitor-like cells.[13] Cultured CFPHs expressed such hepatic progenitor cell markers as CK19, Thy-1, and CD44, but not mature hepatocyte markers such as TO and G6P. We also found that *in vitro*–expanded CFPHs in uPA/SCID mice were able to repopulate the parenchyma, in which they differentiated into mature hepatocytes. FISH (fluorescence *in situ* hybridization) using mouse X chromosome probes showed that the engrafted and propagated CFPHs did not fuse to the mouse cells (data not shown). Thus, replicative CFPHs isolated from postnatal liver are normal, functional hepatocyte progenitor-like cells.

The existence of stem/progenitor cells in the adult liver is controversial.[23-25] In the present study, we showed that the CFPHs expressed CK19, Thy-1, and CD44, but not AFP, in serial culture. Thy-1 antigens are expressed in *h*-hepatic progenitor cells in fetal liver[26] and in rat oval cells,[27] but not in normal adult hepatocytes. We showed that Thy-1-expressing cells were present among the CFPHs at an occupancy of 1%-3%. SHs show greater growth potential than PHs in rats.[12] Other studies have reported that CD44 is a specific marker for rat SHs *in vitro* and *in vivo*, and that its expression level decreases with SH maturation *in vitro*.[17] Moreover, a recent study demonstrated that CD44 was strongly expressed by oval cells in a 2-acetylaminofluorene/partial hepatectomy, a D-galactosamine, and a retrorsine/partial hepatectomy rat model, but not by small hepatocyte-like progenitor cells (SHPCs)[18] that appeared in a retrorsine/partial hepatectomy model.[28] We detected CD44 expression in CFPHs at the plasma membrane. These results suggest that Thy-1 and CD44 may be common markers for both rat and *h*-hepatic progenitor cells.

Mouse embryonic liver stem cell lines differentiate into both hepatocytes and bile ducts in uPA/SCID mice.[29] Like PHs, our CFPHs differentiated into mature hepatocytes, but not into biliary epithelial cells, in uPA/SCID mice. CFPHs are considered to be hepatic progenitor-like cells, like rat SHs[12,30-33] and SHPCs.[28,34] SHPCs are

closely related to SHs; they are small and similar in size,[28,30] and both express CYP3A1 and 2E1 at a low level.[28,32] At 3 weeks posttransplantation, the CFPHs were small in size, had a large nucleus-to-cytoplasm ratio, and expressed *h*CD44, but not *h*CK19. At 10 weeks, the cells became bigger, assumed a morphology similar to that of PH-derived cells, and lost their expression of *h*CD44. The expression of *h*CYP3A4 was quite low (0.15-fold) among CFPHs compared with that of PHs (data not shown). In addition, the distribution of *h*CYP3A4-expressing CFPHs in the pericentral zone was unique: more than two-thirds of CFPHs did not express CYP3A4. In the case of the *h*-PH–chimeric mice, all PHs in the pericentral zone expressed CYP3A4 (data not shown).

Presently, we lack experimental data to explain the expression of *h*CYP3A4 in CFPH-chimeric liver, but CFPHs may require some specific environmental factor(s) for differentiation, which might be absent from mouse liver. Alternatively, some factors that specifically inhibit the differentiation of CFPHs might be present there. CK7-positive *h*-hepatic progenitor cells are present in the livers of uPA/SCID mice transplanted with *h*-postnatal liver-derived PHs,[6] and these small cells are strongly immunoreactive to pan-cytokeratin with scant cytoplasm. The CFPHs were morphologically similar to these cells at 3 weeks posttransplantation, although we were unable to detect CK7-positive cells in either the PH- or CFPH-transplanted chimeric livers. However, CFPHs were *h*CK7-, *h*CK19-, and *h*CD44-positive, at least until 1 day posttransplantation (data not shown).

We reported previously that uPA/SCID livers were nearly completely replaced with young donor PHs at 10 weeks posttransplantation.[5] In contrast, the RIs of our CFPH-chimeric mice were <30% at 9 to 10 weeks. CFPHs were rare in the host liver at 3 weeks posttransplantation, whereas several PHs were observed. The lower RIs of the CFPHs might be attributable to their lower engraftment efficiency.

In conclusion, *h*-hepatocytes in immunodeficient, and liver-injured mice are useful for the study of viral hepatitis. Repopulated *h*-hepatocytes are susceptible to infection with HBV[6-8] and HCV.[4,6] Additionally, *h*-hepatocyte–chimeric mice are usually produced by transplanting fresh[6,7] or cryopreserved hepatocytes,[4,5] but sources of *h*-hepatocytes are limited. Several studies have reported on liver repopulation by *in vitro*–propagated cells from adult and fetal livers, such as immortalized mouse hepatic stem cells,[29] rat SHPCs,[34] immortalized *h*-hepatocytes transfected with full-length HBV,[35] and fetal *h*-epithelial/hepatic progenitor cells.[36,37] However, the RIs in these studies were extremely low (less than a few percent). In the present study, we were able to produce CFPH-chimeric mice with RIs as high as 27%. Thus, CFPHs could be an alternative to *h*-hepatocytes as a source of hepatocytes for transplantation. Moreover, the CFPH-chimeric mice were susceptible to infection with HBV, even though their serum *h*ALB levels were extremely low (10^2-10^3 ng/mL). CFPH-chimeric mice will be useful for studying *h*-HBV and for characterizing *h*-hepatic progenitor cells.

Acknowledgment: We thank H. Kohno, Y. Matsumoto, S. Nagai, A. Tachibana, Y. Yoshizane, and Y. Seo for providing technical assistance. We also thank Dr. K. Ohashi (Tokyo Women's Medical University) for helpful discussion and comments during the preparation of this manuscript.

References

1. Rhim JA, Sandgren EP, Degen JL, Palmiter RD, Brinster RL. Replacement of diseased mouse liver by hepatic cell transplantation. Science 1994; 263:1149-1152.
2. Overturf K, Al-Dhalimy M, Ou CN, Finegold M, Grompe M. Serial transplantation reveals the stem-cell-like regenerative potential of adult mouse hepatocytes. Am J Pathol 1997;151:1273-1280.
3. Laconi E, Oren R, Mukhopadhyay DK, Hurston E, Laconi S, Pani P, et al. Long-term, near-total liver replacement by transplantation of isolated hepatocytes in rats treated with retrorsine. Am J Pathol 1998;153:319-329.
4. Mercer DF, Schiller DE, Elliott JF, Douglas DN, Hao C, Rinfret A, et al. Hepatitis C virus replication in mice with chimeric human livers. Nat Med 2001;7:927-933.
5. Tateno C, Yoshizane Y, Saito N, Kataoka M, Utoh R, Yamasaki C, et al. Near completely humanized liver in mice shows human-type metabolic responses to drugs. Am J Pathol 2004;165:901-912.
6. Meuleman P, Libbrecht L, De Vos R, de Hemptinne B, Gevaert K, Vandekerckhove J, et al. Morphological and biochemical characterization of a human liver in a uPA-SCID mouse chimera. HEPATOLOGY 2005;41: 847-856.
7. Dandri M, Burda MR, Török E, Pollok JM, Iwanska A, Sommer G, et al. Repopulation of mouse liver with human hepatocytes and *in vivo* infection with hepatitis B virus. HEPATOLOGY 2001;33:981-988.
8. Tsuge M, Hiraga N, Takaishi H, Noguchi C, Oga H, Imamura M, et al. Infection of human hepatocyte chimeric mouse with genetically engineered hepatitis B virus. HEPATOLOGY 2005;42:1046-1054.
9. Kocarek TA, Schuetz EG, Guzelian PS. Biphasic regulation of cytochrome P450 2B1/2 mRNA expression by dexamethasone in primary cultures of adult rat hepatocytes maintained on matrigel. Biochem Pharmacol 1994; 48:1815-1822.
10. Arterburn LM, Zurlo J, Yager JD, Overton RM, Heifetz AH. A morphological study of differentiated hepatocytes *in vitro*. HEPATOLOGY 1995;22: 175-187.
11. Tateno C, Yoshizato K. Growth and differentiation in culture of clonogenic hepatocytes that express both phenotypes of hepatocytes and biliary epithelial cells. Am J Pathol 1996;149:1593-1605.
12. Tateno C, Takai-Kajihara K, Yamasaki C, Sato H, Yoshizato K. Heterogeneity of growth potential of adult rat hepatocytes *in vitro*. HEPATOLOGY 2000;31:65-74.
13. Yamasaki C, Tateno C, Aratani A, Ohnishi C, Katayama S, Kohashi T, et al. Growth and differentiation of colony-forming human hepatocytes *in vitro*. J Hepatol 2006;44:749-757.
14. Hino H, Tateno C, Sato H, Yamasaki C, Katayama S, Kohashi T, et al. A long-term culture of human hepatocytes which show a high growth poten-

tial and express their differentiated phenotypes. Biochem Biophys Res Commun 1999;256:184-191.
15. Kocken, JM, de Heer E, Borel Rinkes IH, Sinaasappel M, Terpstra OT, Bruijn JA. Blocking of $\alpha 1\beta 1$ integrin strongly improves survival of hepatocytes in allogeneic transplantation. Lab Invest 1997;77:19-28.
16. Prall F, Nollau P, Neumaier M, Haubeck HD, Drzeniek Z, Helmchen U, et al. CD66a (BGP), an adhesion molecule of the carcinoembryonic antigen family, is expressed in epithelium, endothelium, and myeloid cells in a wide range of normal human tissues. J Histochem Cytochem 1996;44:35-41.
17. Kon J, Ooe H, Oshima H, Kikkawa Y, Mitaka T. Expression of CD44 in rat hepatic progenitor cells. J Hepatol 2006;45:90-98.
18. Yovchev MI, Grozdanov PN, Joseph B, Gupta S, Dabeva MD. Novel hepatic progenitor cell surface markers in the adult rat liver. HEPATOLOGY 2007;45:139-149.
19. Rippin SJ, Hagenbuch B, Meier PJ, Stieger B. Cholestatic expression pattern of sinusoidal and canalicular organic anion transport systems in primary cultured rat hepatocytes. HEPATOLOGY 2001;33:776-782.
20. Sandgren EP, Palmiter RD, Heckel JL, Daugherty CC, Brinster RL, Degen JL. Complete hepatic regeneration after somatic deletion of an albumin-plasminogen activator transgene. Cell 1991;66:245-256.
21. Oinonen T, Lindros KO. Hormonal regulation of the zonated expression of cytochrome P-450 3A in rat liver. Biochem J 1995;309:55-61.
22. Sonnier M, Cresteil T. Delayed ontogenesis of CYP1A2 in the human liver. Eur J Biochem 1998;251:893-898.
23. Sell S. Is there a liver stem cell? Cancer Res 1990;50:3811-3815.
24. Thorgeirsson SS. Hepatic stem cells. Am J Pathol 1993;142:1331-1333.
25. Shafritz DA, Oertel M, Menthena A, Nierhoff D, Dabeva MD. Liver stem cells and prospects for liver reconstitution by transplanted cells. HEPATOLOGY 2006;43(Suppl):89S-98S.
26. Masson NM, Currie IS, Terrace JD, Garden OJ, Parks RW, Ross JA. Hepatic progenitor cells in human fetal liver express the oval cell marker Thy-1. Am J Physiol Gastrointest Liver Physiol 2006;291:G45-G54.
27. Petersen BE, Goff JP, Greenberger JS, Michalopoulos GK. Hepatic oval cells express the hematopoietic stem cell marker Thy-1 in the rat. HEPATOLOGY 1998;27:433-445.
28. Gordon GJ, Coleman WB, Grisham JW. Temporal analysis of hepatocyte differentiation by small hepatocyte-like progenitor cells during liver regeneration in retrorsine-exposed rats. Am J Pathol 2000;157:771-786.
29. Strick-Marchand H, Morosan S, Charneau P, Kremsdorf D, Weiss MC. Bipotential mouse embryonic liver stem cell lines contribute to liver regeneration and differentiate as bile ducts and hepatocytes. Proc Natl Acad Sci U S A 2004;101:8360-8365.
30. Katayama S, Tateno C, Asahara T, Yoshizato K. Size-dependent *in vivo* growth potential of adult rat hepatocytes. Am J Pathol 2001;158:97-105.
31. Mitaka T, Mikami M, Sattler GL, Pitot HC, Mochizuki Y. Small cell colonies appear in the primary culture of adult rat hepatocytes in the presence of nicotinamide and epidermal growth factor. HEPATOLOGY 1992;16:440-447.
32. Asahina K, Shiokawa M, Ueki T, Yamasaki C, Aratani A, Tateno C, et al. Multiplicative mononuclear small hepatocytes in adult rat liver: their isolation as a homogeneous population and localization to periportal zone. Biochem Biophys Res Commun 2006;342:1160-1167.
33. Yoshizato K. Growth potential of adult hepatocytes in mammals: highly replicative small hepatocytes with liver progenitor-like traits. Dev Growth Differ 2007;49:171-184.
34. Gordon GJ, Butz GM, Grisham JW, Coleman WB. Isolation, short-term culture, and transplantation of small hepatocyte-like progenitor cells from retrorsine-exposed rats. Transplantation 2002;73:1236-1243.
35. Brown JJ, Parashar B, Moshage H, Tanaka KE, Engelhardt D, Rabbani E, et al. A long-term hepatitis B viremia model generated by transplanting nontumorigenic immortalized human hepatocytes in Rag-2-deficient mice. HEPATOLOGY 2000;31:173-181.
36. Malhi H, Irani AN, Gagandeep S, Gupta S. Isolation of human progenitor liver epithelial cells with extensive replication capacity and differentiation into mature hepatocytes. J Cell Sci 2002;115:2679-2688.
37. Nowak G, Ericzon BG, Nava S, Jaksch M, Westgren M, Sumitran-Holgersson S. Identification of expandable human hepatic progenitors which differentiate into mature hepatic cells *in vivo*. Gut 2005;54:972-979.

Journal of General Virology (2008), 89, 2108–2113 DOI 10.1099/vir.0.83658-0

Establishment of an infectious genotype 1b hepatitis C virus clone in human hepatocyte chimeric mice

Takashi Kimura,[1,2] Michio Imamura,[1,2] Nobuhiko Hiraga,[1,2] Tsuyoshi Hatakeyama,[1,2] Daiki Miki,[1,2] Chiemi Noguchi,[1,2] Nami Mori,[1,2] Masataka Tsuge,[1,2] Shoichi Takahashi,[1,2] Yoshifumi Fujimoto,[1,2] Eiji Iwao,[3] Hidenori Ochi,[2,4] Hiromi Abe,[1,2,4] Toshiro Maekawa,[4] Keiko Arataki,[5] Chise Tateno,[2,6] Katsutoshi Yoshizato,[2,6] Takaji Wakita,[7] Toru Okamoto,[8] Yoshiharu Matsuura[8] and Kazuaki Chayama[1,2,4]

Correspondence
Kazuaki Chayama
chayama@hiroshima-u.ac.jp

[1]Department of Medicine and Molecular Science, Division of Frontier Medical Science, Programs for Biomedical Research, Graduate School of Biomedical Sciences, Hiroshima University, Hiroshima, Japan

[2]Liver Research Project Center, Hiroshima University, Hiroshima, Japan

[3]Research Division, Mitsubishi Tanabe Pharma Corporation, Osaka, Japan

[4]Laboratory for Liver Disease, SNP Research Center, Institute of Physical and Chemical Research (RIKEN), Yokohama, Japan

[5]Hirosimakinen-Hospital, Internal Medicine, Hiroshima, Japan

[6]Developmental Biology Laboratory, Department of Biological Science, Graduate School of Science, Hiroshima University, Higashihiroshima, Japan

[7]Department of Virology II, National Institute of Infectious Diseases, Shinjuku-ku, Japan

[8]Department of Molecular Virology, Research Institute for Microbial Diseases, Osaka University, Osaka, Japan

The establishment of clonal infection of hepatitis C virus (HCV) in a small-animal model is important for the analysis of HCV virology. A previous study developed models of molecularly cloned genotype 1a and 2a HCV infection using human hepatocyte-transplanted chimeric mice. This study developed a new model of molecularly cloned genotype 1b HCV infection. A full-length genotype 1b HCV genome, HCV-KT9, was cloned from a serum sample from a patient with severe acute hepatitis. The chimeric mice were inoculated intrahepatically with *in vitro*-transcribed HCV-KT9 RNA. Inoculated mice developed viraemia at 2 weeks post-infection, and this persisted for more than 6 weeks. Passage experiments indicated that the sera of these mice contained infectious HCV. Interestingly, a similar clone, HCV-KT1, in which the poly(U/UC) tract was 29 nt shorter than in HCV-KT9, showed poorer *in vivo* infectivity and replication ability. An *in vitro* study showed that no virus was produced in the culture medium from HCV-KT9-transfected cells. In conclusion, this study developed a genetically engineered genotype 1b HCV-infected mouse. This mouse model will be useful for the study of HCV virology, particularly the mechanism underlying the variable resistance of HCV genotypes to interferon therapy.

Received 13 December 2007
Accepted 14 May 2008

INTRODUCTION

Hepatitis C virus (HCV), a positive-sense, single-stranded RNA virus, infects and replicates efficiently only in the hepatocytes of humans and chimpanzees. There are many genotypes of HCV distributed worldwide (Simmonds *et al.*, 1993); among them genotype 1b is the major genotype in Asia, including Japan, and is known to be one of the most resistant genotypes to interferon (IFN) therapy (Fried *et al.*, 2002). Until recently, studies of HCV replication have long been hampered by the lack of a virus culture system. The development of HCV replicon systems has allowed the

The GenBank/EMBL/DDBJ accession numbers for the sequences of HCV-KT9 and HCV-KT1 determined in this work are AB435162 and AB426117, respectively.

0008-3658 © 2008 SGM *Printed in Great Britain*

study of the mechanisms of replication of HCV (Lohmann *et al.*, 1999). However, these replicons lack structural proteins, do not replicate efficiently without adaptive mutations and do not produce infectious virions. Recently, it was reported that the genotype 2a full-length JFH-1 genome replicated efficiently in Huh7 cells without adaptive mutations and produced virions that were infectious for both naïve cells and chimpanzees, as well as for a human hepatocyte-transplanted chimeric mouse (Wakita *et al.*, 2005; Zhong *et al.*, 2005; Lindenbach *et al.*, 2006). To date, five full-length genotype 1b clones, HCV-N (Beard *et al.*, 1999), Con-1 (Bukh *et al.*, 2002), HCV-J4 (Okamoto *et al.*, 1992), HCV-CG1b (Thomson *et al.*, 2001) and HCV-BK (Takamizawa *et al.*, 1991), have been demonstrated to be infectious by intrahepatic inoculation of transcribed HCV RNA into the liver of chimpanzees. Among these, only the HCV-CG1b genome is reported to produce HCV particles when transfected into Huh7 cells (Heller *et al.*, 2005).

Although the chimpanzee is a useful animal model for the study of HCV infection, there are ethical restrictions on the use of this animal. Instead, Mercer *et al.* (2001) developed a useful small-animal model for the study of HCV infection using chimeric urokinase-type plasminogen activator (uPA)/severe combined immunodeficiency (SCID) mice (which are immunodeficient and undergo liver failure) with engrafted human hepatocytes. This HCV-infected mouse model is reported to be useful for evaluating anti-HCV drugs such as IFN-α and anti-NS3 protease (Kneteman *et al.*, 2006). We have previously described methods to improve the replacement levels of human hepatocytes in this mouse model (Tateno *et al.*, 2004) and we have developed a reverse genetics system for hepatitis B virus (Tsuge *et al.*, 2005) and HCV (Hiraga *et al.*, 2007). In the present study, we report the establishment of an infectious genotype 1b HCV clone that infects and replicates efficiently in human hepatocyte chimeric mice.

METHODS

Cloning of infectious genotype 1b HCV isolate. Serum samples were obtained from a 43-year-old physician who developed severe acute hepatitis after needle stick exposure from a patient with chronic hepatitis C. On admission, the serum total bilirubin concentration was 10.0 mg dl^{-1} and the prothrombin time was 40 %. The patient tested positive for HCV antibodies by a third-generation radioimmunoassay (Ortho-Clinical Diagnostics) and for HCV RNA by RT-PCR. Serum HCV RNA was quantified using an Amplicor Monitor HCV test (Roche Diagnostics). The HCV RNA titre was 2.5×10^6 copies ml^{-1} on admission and then decreased gradually. Fig. 1 shows the serial changes in alanine aminotransferase (ALT) as a measure of liver function and HCV RNA levels in this patient. Serum samples obtained in the early phase of infection were used for cloning the full-length genome.

RNA extraction, cDNA synthesis, plasmid construction and RNA transcription. Total RNA was extracted from 100 µl serum samples using SepaGene RV-R (Sanko Junyaku) and reverse transcribed with random hexamers and ReverTra Ace reverse transcriptase (Toyobo) according to the manufacturer's instructions. PCR primers were designed based on the sequence of HCV-Con1 (GenBank accession no. AJ238799; Bukh *et al.*, 2002). Five overlapping cDNA segments (nt 1–2292, 2269–6715, 6696–9094, 7564–9404 and 9361–9605; nucleotide numbers are those of HCV-Con1) were amplified by PCR with TaKaRa LA *Taq* polymerase (Takara Biochemicals) using the above cDNA. Amplified products were separated by agarose gel electrophoresis. Nucleotide sequences were determined using a Big Dye Terminator Mix Cycle Sequencing kit (Applied Biosystems Japan) with an automated DNA sequencer (model 310; PE Biosystems). We corrected the nucleotide sequences of the obtained clones by site-directed mutagenesis and made them identical to the nucleotide sequences obtained by direct sequencing. Naturally occurring restriction enzyme cutting sites were utilized to clone each segment. We utilized the vector pBR322 and created a multiple-cloning site under the control of the T7 promoter by ligating a linker at restriction enzyme cutting sites as they appeared in order from 5′ to 3′ in the HCV sequences (Fig. 2a). Each segment of HCV was cloned into this vector to generate the full-length clones. The HCV-KT9 clone was established using the 3′-terminal fragment with the longest poly(U/UC) tract length (115 nt), which should have a high replication ability (Friebe & Bartenschlager, 2002; Yi & Lemon, 2003; You & Rice, 2008). A clone with a shorter poly(U/UC) tract length (86 nt), HCV-KT1, was also generated. A polymerase-deficient mutant with an amino acid substitution in the GDD motif (GDD→GND; HCV-KT9-GND) was generated using a Quick Change Site-Directed Mutagenesis kit (Stratagene). After digesting the plasmid with *Xba*I (New England BioLabs) at the 3′ end of the HCV cDNA, HCV RNA was transcribed using T7 RNA polymerase (MEGAscript; Ambion) at 37 °C for 3 h in a 100 µl reaction mixture, according to the manufacturer's instructions. The RNA was analysed using denaturing agarose gel electrophoresis and kept at −80 °C until use.

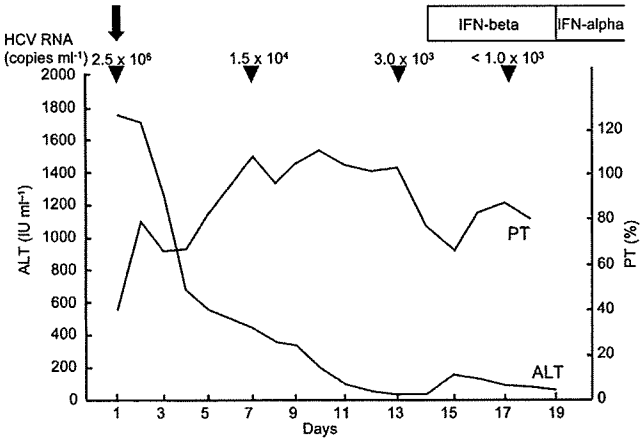

Fig. 1. Clinical course of a patient with severe acute hepatitis C. Alanine aminotransferase (ALT) and prothrombin time (PT) are shown from the day of admission (day 1). The patient was treated daily with 10^6 U IFN-β intravenously for 5 days, followed by 10^6 U IFN-α intramuscularly three times a week for 6 months. HCV RNA was measured on days 1, 7, 13 and 17 (arrowheads). A serum sample was taken on day 1 (arrow) and used to clone the full-length HCV genome.

Construction of a phylogenetic tree. A phylogenetic tree was constructed based on the entire nucleotide sequences of 26 full-length genotype 1b clones plus HCV-KT9. The total number of synonymous and non-synonymous substitutions among the nucleotide sequences was estimated using the method of Gojobori *et al.* (1982) and a phylogenetic tree was constructed by the neighbour-joining method (Saitou & Nei, 1987).

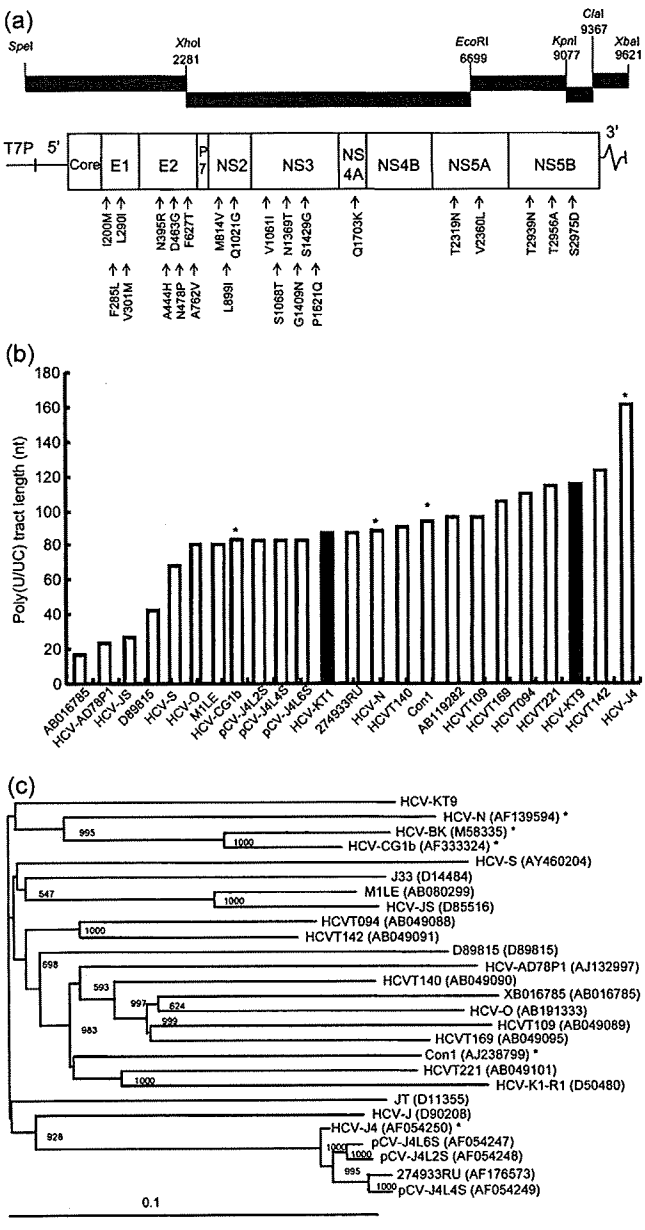

Fig. 2. (a) Schematic diagram of the organization of the cDNA clone HCV-TK9. The T7 RNA promoter (T7P) is located immediately upstream of the HCV genome. Restriction enzyme sites that were used to create clone HCV-KT9 are labelled according to their nucleotide position within the HCV sequence. Amino acid sequences unique to HCV-KT9 compared with 26 other HCV genotype 1b isolates are indicated at the bottom of the figure, with the position of the repaired amino acid residues noted within the polyprotein. (b) Length of the poly(U/UC) tracts of HCV-KT1, HCV-KT9 and 22 other HCV genotype 1b clones reported previously. Asterisks indicate clones confirmed to be infectious by experiments using chimpanzees. (c) Phylogenetic tree constructed with HCV-KT9 and 26 genotype 1b HCV whole-genome sequences. Bar, number of nucleotide substitutions per site. Asterisks indicate clones confirmed to be infectious in experiments using chimpanzees.

Intrahepatic injection experiments in human hepatocyte chimeric mice. We used methods described previously (Tateno *et al.*, 2004) to generate uPA$^{+/+}$/SCID$^{+/+}$ mice and transplant human hepatocytes. All mice used in this study were transplanted with frozen human hepatocytes obtained from the same donor. Mouse serum concentrations of human serum albumin (HSA) correlate with the repopulation index and were measured as described previously (Tateno *et al.*, 2004). Intrahepatic injection of RNA, extraction of serum samples and euthanasia were performed under ether anaesthesia. Briefly, 500 µl RNA solution containing 30 µg transcribed HCV RNA was injected into the liver of anaesthetized chimeric mice through a small abdominal incision. RNA extraction from mouse serum samples, quantification of HCV RNA and nested PCR were performed as described previously (Hiraga *et al.*, 2007). All animal protocols described in this study were performed in accordance with the guidelines of the local committee for animal experiments and under the approval of the Ethics Review Committee for Animal Experimentation of the Graduate School of Biomedical Sciences, Hiroshima University.

Cell culture, RNA transfection and measurement of HCV core antigen. The human hepatoma cell line Huh7 was maintained in Dulbecco's modified Eagle's medium (Sigma) containing 10% fetal calf serum. RNA transfection and measurement of HCV core antigen in the culture medium were performed as described previously (Wakita *et al.*, 2005).

Statistical analysis. The infectious ratio of chimeric mice was compared and the differences assessed using a χ^2 test. Differences in HCV RNA replication ability *in vitro* were analysed statistically by one-way analysis of variance followed by Scheffe's test. A P value of less than 0.05 was considered statistically significant.

RESULTS

Characteristics of genotype 1b clones HCV-KT9 and HCV-KT1

The entire genome of HCV cDNA was assembled from five DNA fragments (Fig. 2a). We obtained 24 3′-extremity clones with different poly(U/UC) tract lengths. We selected the clone with the longest (U/UC) tract because a previous study indicated that the length of poly(U/UC) tract correlates with HCV replication in an HCV replicon system (Friebe & Bartenschlager, 2002; Yi & Lemon, 2003; You & Rice, 2008). The length of the poly(U/UC) tract in the longest 3′ clone was 115 nt. The entire genome length of the HCV-KT9 clone using this longest 3′ clone was 9621 nt. We also generated the clone HCV-KT1 with a shorter (86 nt) poly (U/UC) tract to compare the replication abilities of these clones. The lengths of the poly(U/UC) tracts of 22 clones deposited in GenBank are shown in Fig. 2(b). All infectious clones had a poly(U/UC) tract longer than 80 nt. Fig. 2(c) shows a phylogenetic tree constructed using the nucleotide sequences of the 26 full-length genotype 1b clones published to date. Interestingly, the sequence of HCV-KT9 was closest to that of HCV-CG1b (GenBank accession no. AF333324), which has been reported to be infectious, and formed a cluster with two other infectious clones, HCV-N (Beard *et al.*, 1999) and HCV-BK (Takamizawa *et al.*, 1991). We compared the amino acid

sequences of HCV-KT9 with an alignment of the sequences of the 26 other genotype 1b strains. All HCV full-length clones reported from Japan were included in these 26 strains. Based on these comparisons, we identified 25 aa unique to HCV-KT9 (Fig. 2a). We found that the amino acid sequence of the IFN sensitivity-determining region in the NS5A region, which has been suggested to mediate IFN resistance via interaction with the cellular protein kinase R (Enomoto *et al.*, 1996; Gale *et al.*, 1997), was that of the wild-type.

Intrahepatic injection of HCV-KT1 and HCV-KT9 RNAs into human hepatocyte chimeric mice

In the next experiments, 30 μg *in vitro*-transcribed RNA of HCV-KT1, HCV-KT9 or HCV-KT9-GND was injected into the livers of chimeric mice. Eight of 10 (80%) HCV-KT9-injected mice developed measurable viraemia at 2 weeks post-inoculation (Table 1 and Fig. 3), with the HCV RNA titre reaching 1.1×10^6 to 8.8×10^6 copies ml^{-1} at 6 weeks post-inoculation (Fig. 3). To check for the presence of infectious HCV in the serum of HCV-KT9-infected mice, each of five naïve mice was injected with 10 μl serum sample (containing 3.5×10^5 copies of HCV) obtained from an HCV-KT9-infected mouse 6 weeks after inoculation. All five naïve mice became positive for HCV RNA, as confirmed by nested PCR, at 2 weeks post-inoculation and two mice developed persistent viraemia (Fig. 4). These results indicated that the serum of HCV-KT9-injected mice contained infectious HCV. In contrast to HCV-KT9, none of the three mice injected with HCV-KT9-GND RNA developed viraemia (Table 1). These results indicated that HCV-KT9 replicates efficiently in mice livers and produces infectious virus continuously. On the other hand, only one out of seven HCV-KT1-injected mice (14%) developed measurable viraemia (Table 1 and Fig. 3). The level of viraemia was low in this HCV-KT1-infected mouse, HCV RNA was negative by nested PCR at 2 weeks after inoculation and the titre was only 2.2×10^4 copies ml^{-1} at 4 weeks post-inoculation (Fig. 3). These results confirmed the importance of the poly(U/UC) tract length in experimentally induced viraemia.

The nucleotide and amino acid sequences of the viral genome isolated from an HCV-KT9-injected mouse (Fig. 3) at 6 weeks after RNA injection were identical to the injected HCV-KT9 (data not shown). We tried to reclone the poly(U/UC) tract in the HCV-KT1-infected mouse, but it was impossible to reamplify the HCV cDNA using the remaining small amount of serum.

Table 1. Correlation between length of the poly(U/UC) tract and HCV infection

Clone	Length of poly(U/UC) tract	Number of mice			Infection ratio
		Infected	Not infected	Total	
HCV-KT1	86	1	6	7	14%
HCV-KT9	115	8	2	10	80%*
HCV-KT9-GND	115	0	3	3	0%

*P=0.015, compared with HCV-KT1.

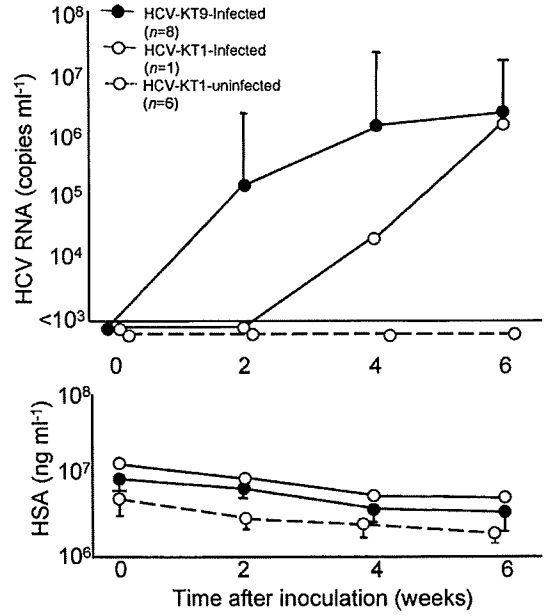

Fig. 3. Changes in HCV RNA levels and HSA concentrations in the sera of mice infected with clonal HCV. Mice were inoculated intrahepatically with 30 μg *in vitro*-transcribed HCV RNA. Eight of the ten HCV-KT9-infected mice (80%), one of the seven HCV-KT1-infected mice (14%) and none of the three HCV-KT9-GND-infected mice became positive for HCV RNA. The results for six HCV-KT1-uninfected mice are also shown. Mice serum samples were obtained every 2 weeks post-infection for analysis of HCV RNA titres. Data are shown as mean ± SD.

Analysis of virus production from HCV-KT9-transfected cells

Next, we evaluated the ability of the HCV-KT9 clone to replicate in transfected Huh7 cells. In these experiments, we used JFH-1 RNA, which is known to replicate efficiently in cell cultures, as control (Wakita *et al.*, 2005). Core protein was secreted efficiently from JFH-1 RNA-transfected Huh7 cells. In contrast, we did not observe any measurable levels of core protein in the supernatant of HCV-KT9-transfected cells (Fig. 5), suggesting a minimal replication ability of HCV-KT9 to produce and release virus into the supernatant.

DISCUSSION

In this study, we described the establishment of a genotype 1b clone, HCV-KT9, that replicated efficiently following injection of the transcribed RNA into chimeric mouse liver.

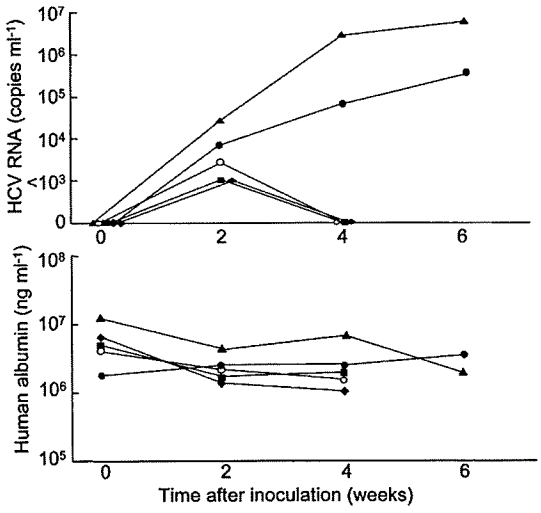

Fig. 4. Passage experiments of HCV in naïve chimeric mice. Five naïve chimeric mice were inoculated intravenously with 10 µl serum sample (containing 3.5×10^5 copies HCV) obtained from an HCV-KT9-infected mouse at week 6 post-inoculation. Serum samples were obtained at the indicated time intervals for the measurement of HCV RNA levels and HSA concentrations. Data represent the changes in five individual mice.

The key factor that determines the infectivity of HCV clones has not yet been established. We previously established a clone from HCV that replicated in a chimeric mouse after injection of serum from a chronically HCV-infected patient. However, we did not observe viraemia after intrahepatic injection of the transcribed RNA from this clone (unpublished results). In contrast, injection of HCV-KT9 RNA in the present study resulted in viraemia in eight out of ten mice (80 %). The fact that the nucleotide and amino acid sequences of the virus recovered from the infected mice were identical to those of the HCV-KT9 clone indicated that no adaptive mutation was necessary for this clone to replicate in the chimeric mouse.

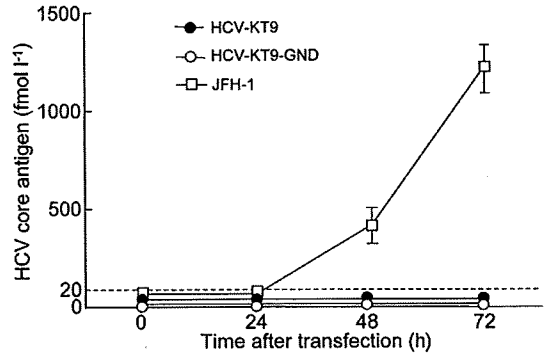

Fig. 5. Time-course studies of HCV core protein secretion into the culture medium of HCV RNA-transfected cells. Huh7 cells were transfected with 10 µg HCV-KT9, HCV-KT9-GND or JFH-1 RNA. HCV core antigen in the culture medium was measured at 24, 48 and 72 h after transfection. Data are shown as mean ± SD of HCV core protein levels obtained from three independent transfection experiments.

Interestingly, the clone was obtained from a patient with severe acute hepatitis. This is similar to JFH-1, an HCV clone with a strong replication ability in cultured cell lines, chimpanzees and chimeric mice, which was cloned from serum samples of a patient who developed acute fulminant hepatitis with a high virus titre (Wakita *et al.*, 2005). A virus that replicates in the early stage of infection may have strong replication ability, which may be lost in the chronic phase of infection.

A key amino acid substitution may be present in one (or some) of the amino acids unique to this clone (Fig. 2a). We also showed that clone HCV-KT1, which differs from HCV-KT9 only in the length of the poly(U/UC) tract, had a poorer replication ability in mice (Table 1 and Fig. 3). However, there is a possibility that a shorter poly(U/UC) tract only slows down the rate of infection, as the HCV RNA titre in the HCV-KT1-infected mouse at 6 weeks after inoculation was similar to that in HCV-KT9-infected mice (Fig. 3). It has been reported that the length and composition of the poly(U/UC) tract is important for the replication of HCV replicons (Friebe & Bartenschlager, 2002; Yi & Lemon, 2003; You & Rice, 2008). However, no replication advantage of a poly(U/UC) tract longer than 86 bp was revealed in this study. This may be due to differences *in vitro* and *in vivo*, where the innate immune response against the virus may be more robust than in cell culture.

As shown in the present study, reverse genetics of HCV has become available for studies of HCV replication. The important factors for virus replication suggested above can be analysed further using this system.

We also examined the response of HCV-KT9-infected mice to IFN treatment. Three HCV-KT9-infected mice were treated with daily intramuscular injections of 1000 IU IFN-α (g body weight)$^{-1}$ for 2 weeks. This regimen resulted in a reduction in HCV RNA levels of only 1.0 log copies ml^{-1} (data not shown). These results are consistent with our previous study, which showed a similar low-level reduction in HCV RNA in mice infected with a genotype 1a clone, and differ from our previous results in mice infected with HCV genotype 2a, which became negative for HCV RNA following daily treatment with 1000 IU IFN-α (g body weight)$^{-1}$ for 2 weeks (Hiraga *et al.*, 2007). These results are in agreement with our clinical experience that genotype 1 is more resistant to IFN therapy than genotype 2. As shown in the present study and previously (Hiraga *et al.*, 2007), reverse genetics of HCV with three genotypes, 1a, 1b and 2a, is now available. By recombination of these clones or the establishment of mutants with nucleotide and amino acid sequences similar to each other, it may be possible to clarify the mechanism underlying the variability in susceptibility of HCV genotypes to IFN.

In this study, HCV-KT9 showed no virus production ability *in vitro*. Recently, Kato *et al.* (2007) reported that the genotype 1b HCV clone CG1b replicated in Huh7.5.1 cells and produced infectious HCV. It will be of interest to create chimeric viruses of HCV-KT9 and HCV-CG1b, and to determine the mutations that are important for virus production *in vitro*.

In summary, we established an infection model of a genotype 1b HCV clone using human hepatocyte chimeric mice. This model will be useful for studies of HCV replication, particularly the mechanism underlying the variable resistance of HCV genotypes to IFN therapy.

ACKNOWLEDGEMENTS

The authors thank Rie Akiyama and Kana Kunihiro for their technical help and Dr Francis V. Chisari for providing the Huh7.5.1 cells. This work was supported in part by Grants-in-Aid for scientific research and development from the Ministry of Education, Sports, Culture and Technology and the Ministry of Health, Labor and Welfare, Japan.

REFERENCES

Beard, M. R., Abell, G., Honda, M., Carroll, A., Gartland, M., Clarke, B., Suzuki, K., Lanford, R., Sangar, D. V. & Lemon, S. M. (1999). An infectious molecular clone of a Japanese genotype 1b hepatitis C virus. *Hepatology* **30**, 316–324.

Bukh, J., Pietschmann, T., Lohmann, V., Krieger, N., Faulk, K., Engle, R. E., Govindarajan, S., Shapiro, M., St Claire, M. & other authors (2002). Mutations that permit efficient replication of hepatitis C virus RNA in Huh-7 cells prevent productive replication in chimpanzees. *Proc Natl Acad Sci U S A* **99**, 14416–14421.

Enomoto, N., Sakuma, I., Asahina, Y., Kurosaki, M., Murakami, T., Yamamoto, C., Ogura, Y., Izumi, N., Marumo, F. & other authors (1996). Mutations in the nonstructural protein 5A gene and response to interferon in patients with chronic hepatitis C virus 1b infection. *N Engl J Med* **334**, 77–81.

Friebe, P. & Bartenschlager, R. (2002). Genetic analysis of sequences in the 3′ nontranslated region of hepatitis C virus that are important for RNA replication. *J Virol* **76**, 5326–5338.

Fried, M. W., Shiffman, M. L., Reddy, K. R., Smith, C., Marinos, G., Goncales, F. L., Jr, Haussinger, D., Diago, M., Carosi, G. & other authors (2002). Peginterferon alfa-2a plus ribavirin for chronic hepatitis C virus infection. *N Engl J Med* **347**, 975–982.

Gale, M. J., Jr, Korth, M. J., Tang, N. M., Tan, S. L., Hopkins, D. A., Dever, T. E., Polyak, S. J., Gretch, D. R. & Katze, M. G. (1997). Evidence that hepatitis C virus resistance to interferon is mediated through repression of the PKR protein kinase by the nonstructural 5A protein. *Virology* **230**, 217–227.

Gojobori, T., Ishii, K. & Nei, M. (1982). Estimation of average number of nucleotide substitutions when the rate of substitution varies with nucleotide. *J Mol Evol* **18**, 414–423.

Heller, T., Saito, S., Auerbach, J., Williams, T., Moreen, T. R., Jazwinski, A., Cruz, B., Jeurkar, N., Sapp, R. & other authors (2005). An in vitro model of hepatitis C virion production. *Proc Natl Acad Sci U S A* **102**, 2579–2583.

Hiraga, N., Imamura, M., Tsuge, M., Noguchi, C., Takahashi, S., Iwao, E., Fujimoto, Y., Abe, H., Maekawa, T. & other authors (2007). Infection of human hepatocyte chimeric mouse with genetically engineered hepatitis C virus and its susceptibility to interferon. *FEBS Lett* **581**, 1983–1987.

Kato, T., Matsumura, T., Heller, T., Saito, S., Sapp, R. K., Murthy, K., Wakita, T. & Liang, T. J. (2007). Production of infectious hepatitis C virus of various genotypes in cell cultures. *J Virol* **81**, 4405–4411.

Kneteman, N. M., Weiner, A. J., O'Connell, J., Collett, M., Gao, T., Aukerman, L., Kovelsky, R., Ni, Z. J., Zhu, Q. & other authors (2006). Anti-HCV therapies in chimeric scid-Alb/uPA mice parallel outcomes in human clinical application. *Hepatology* **43**, 1346–1353.

Lindenbach, B. D., Meuleman, P., Ploss, A., Vanwolleghem, T., Syder, A. J., McKeating, J. A., Lanford, R. E., Feinstone, S. M., Major, M. E. & other authors (2006). Cell culture-grown hepatitis C virus is infectious in vivo and can be recultured in vitro. *Proc Natl Acad Sci U S A* **103**, 3805–3809.

Lohmann, V., Korner, F., Koch, J., Herian, U., Theilmann, L. & Bartenschlager, R. (1999). Replication of subgenomic hepatitis C virus RNAs in a hepatoma cell line. *Science* **285**, 110–113.

Mercer, D. F., Schiller, D. E., Elliott, J. F., Douglas, D. N., Hao, C., Rinfret, A., Addison, W. R., Fischer, K. P., Churchill, T. A. & other authors (2001). Hepatitis C virus replication in mice with chimeric human livers. *Nat Med* **7**, 927–933.

Okamoto, H., Kojima, M., Okada, S., Yoshizawa, H., Iizuka, H., Tanaka, T., Muchmore, E. E., Peterson, D. A., Ito, Y. & other authors (1992). Genetic drift of hepatitis C virus during an 8.2-year infection in a chimpanzee: variability and stability. *Virology* **190**, 894–899.

Saitou, N. & Nei, M. (1987). The neighbor-joining method: a new method for reconstructing phylogenetic trees. *Mol Biol Evol* **4**, 406–425.

Simmonds, P., Holmes, E. C., Cha, T. A., Chan, S. W., McOmish, F., Irvine, B., Beall, E., Yap, P. L., Kolberg, J. & other authors (1993). Classification of hepatitis C virus into six major genotypes and a series of subtypes by phylogenetic analysis of the NS-5 region. *J Gen Virol* **74**, 2391–2399.

Takamizawa, A., Mori, C., Fuke, I., Manabe, S., Murakami, S., Fujita, J., Onishi, E., Andoh, T., Yoshida, I. & other authors (1991). Structure and organization of the hepatitis C virus genome isolated from human carriers. *J Virol* **65**, 1105–1113.

Tateno, C., Yoshizane, Y., Saito, N., Kataoka, M., Utoh, R., Yamasaki, C., Tachibana, A., Soeno, Y., Asahina, K. & other authors (2004). Near completely humanized liver in mice shows human-type metabolic responses to drugs. *Am J Pathol* **165**, 901–912.

Thomson, M., Nascimbeni, M., Gonzales, S., Murthy, K. K., Rehermann, B. & Liang, T. J. (2001). Emergence of a distinct pattern of viral mutations in chimpanzees infected with a homogeneous inoculum of hepatitis C virus. *Gastroenterology* **121**, 1226–1233.

Tsuge, M., Hiraga, N., Takaishi, H., Noguchi, C., Oga, H., Imamura, M., Takahashi, S., Iwao, E., Fujimoto, Y. & other authors (2005). Infection of human hepatocyte chimeric mouse with genetically engineered hepatitis B virus. *Hepatology* **42**, 1046–1054.

Wakita, T., Pietschmann, T., Kato, T., Date, T., Miyamoto, M., Zhao, Z., Murthy, K., Habermann, A., Krausslich, H. G. & other authors (2005). Production of infectious hepatitis C virus in tissue culture from a cloned viral genome. *Nat Med* **11**, 791–796.

Yi, M. & Lemon, S. M. (2003). 3′ Nontranslated RNA signals required for replication of hepatitis C virus RNA. *J Virol* **77**, 3557–3568.

You, S. & Rice, C. M. (2008). 3′ RNA elements in hepatitis C virus replication: kissing partners and long poly(U). *J Virol* **82**, 184–195.

Zhong, J., Gastaminza, P., Cheng, G., Kapadia, S., Kato, T., Burton, D. R., Wieland, S. F., Uprichard, S. L., Wakita, T. & other authors (2005). Robust hepatitis C virus infection *in vitro*. *Proc Natl Acad Sci U S A* **102**, 9294–9299.

Risk Factors for Hepatocellular Carcinoma in a Japanese Population: A Nested Case-Control Study

Waka Ohishi,[1] Saeko Fujiwara,[1] John B. Cologne,[2] Gen Suzuki,[1,5] Masazumi Akahoshi,[1] Nobuo Nishi,[3] Ikuno Takahashi,[1] and Kazuaki Chayama[4]

Departments of [1]Clinical Studies, [2]Statistics, and [3]Epidemiology, Radiation Effects Research Foundation; [4]Department of Medicine and Molecular Science, Division of Frontier Medical Science, Programs for Biomedical Research, Graduate School of Biomedical Sciences, Hiroshima University, Hiroshima, Japan; and [5]Department of Environmental Health, National Institute of Public Health, Wako, Japan

Abstract

Background: **Epidemiologic studies have shown effects of lifestyle-related factors on risk for hepatocellular carcinoma. However, few cohort studies have incorporated, in a strict and in-depth manner, hepatitis B virus (HBV) and hepatitis C virus (HCV) infections or investigated synergism between such factors.**

Methods: **We conducted a nested case-control study using sera stored before hepatocellular carcinoma diagnosis in the longitudinal cohort of atomic bomb survivors. The study included 224 hepatocellular carcinoma cases and 644 controls that were matched to the cases on gender, age, city, time of serum storage, and method of serum storage, and countermatched on radiation dose.**

Results: **Univariate analysis showed that HBV and HCV infections, alcohol consumption, smoking habit, body mass index (BMI), and diabetes mellitus were associated with increased hepatocellular carcinoma risk, whereas coffee drinking was associated with decreased hepatocellular carcinoma risk. Multivariate relative risks of hepatocellular carcinoma (95% confidence interval) were 45.8 (15.2-138), 101 (38.7-263), 70.7 (8.3-601), 4.36 (1.48-13.0), and 4.57 (1.85-11.3), for HBV infection alone, HCV infection alone, both HBV and HCV infections, alcohol consumption of ≥40 g of ethanol per day, and BMI of >25.0 kg/m^2 10 years before diagnosis, respectively. HBV and HCV infection and BMI of >25.0 kg/m^2 remained independent risk factors even after adjusting for severity of liver fibrosis. Among HCV-infected individuals, the relative risk of hepatocellular carcinoma for a 1 kg/m^2 increase in BMI was 1.39 (P = 0.003).**

Conclusions: **To limit the risk for hepatocellular carcinoma, control of excess weight may be crucial for individuals with chronic liver disease, especially those with chronic hepatitis C.** (Cancer Epidemiol Biomarkers Prev 2008;17(4):846–54)

Introduction

Hepatocellular carcinoma is one of the most common cancers worldwide. Chronic infections with hepatitis B virus (HBV) or with hepatitis C virus (HCV) are recognized as critically important risk factors for hepatocellular carcinoma. In addition, a large number of epidemiologic studies have shown that environmental factors such as dietary aflatoxin, smoking, alcohol consumption, and oral contraceptive intake are associated with increased risk for hepatocellular carcinoma (1, 2). It is generally considered that effects of these environmental factors are modified by gender, age, and race of patients (2-4).

Obesity and diabetes mellitus have recently received increased attention as risk factors for hepatocellular carcinoma (5-9). A large number of epidemiologic studies have shown that obesity and diabetes mellitus increase risks of a variety of cancers, including colon, renal, prostate, postmenopausal breast, and ovarian, in Asian and Western countries (7, 10, 11). Several recent epidemiologic studies indicated that obesity might be associated with an increased risk for hepatocellular carcinoma, but few cohort studies have incorporated HBV and HCV infection status in a strict and in-depth manner. A recent study of liver cirrhosis showed that, although obesity [body mass index (BMI), >30 kg/m^2] is an independent risk factor for hepatocellular carcinoma among patients with alcoholic cirrhosis or cryptogenic cirrhosis, it is not a significant risk factor for hepatocellular carcinoma in patients with chronic HBV and/or HCV infections (12).

Compared with viral etiologic factors, alcohol consumption, smoking, obesity, and diabetes mellitus may have less effect on hepatocellular carcinoma occurrence (13, 14); however, most epidemiologic studies have indicated that such factors promote development from chronic hepatitis to hepatocellular carcinoma (6, 8). Alcohol consumption, obesity, and diabetes mellitus have been shown to be involved in the progression of liver fibrosis; it is possible that liver fibrosis results from advanced oxidative stress due to hepatic steatosis and iron overload (15-17). Liver cirrhosis characterized by severe liver fibrosis may underlie the occurrence of hepatocellular carcinoma, specifically in the presence of chronic hepatitis C, nonalcoholic steatohepatitis, and

Received 11/16/07; revised 1/15/08; accepted 2/1/08.

Grant support: Japanese Ministry of Health, Labor and Welfare grant H16-Cancer Prevention-012 and Japanese Ministry of Education, Culture, Sports, Science and Technology grant 18590626.

The costs of publication of this article were defrayed in part by the payment of page charges. This article must therefore be hereby marked *advertisement* in accordance with 18 U.S.C. Section 1734 solely to indicate this fact.

Requests for reprints: Waka Ohishi, Department of Clinical Studies, Radiation Effects Research Foundation, 5-2 Hijiyama Park, Minami-ku, Hiroshima 732-0815, Japan. Phone: 81-82-261-3131; Fax: 81-82-261-3259. E-mail: nwaka@rerf.or.jp

Copyright © 2008 American Association for Cancer Research.

doi:10.1158/1055-9965.EPI-07-2806

alcoholic liver diseases (3, 8). On the other hand, several recent large-scale studies have indicated that coffee drinking suppressed the progression of liver fibrosis and inhibited the development of hepatocellular carcinoma (18, 19).

The fact that liver cirrhosis is not a necessary condition for hepatocellular carcinoma occurrence was already known, not only from clinical findings but also from genetic findings. Among hepatocellular carcinoma cases with HBV, a part of the HBV genome has been shown to be integrated into the host's intracellular DNA, thereby causing hepatocellular carcinoma (20). Among hepatocellular carcinoma cases with HCV, the HCV core protein seems to directly contribute to the mechanism of carcinogenesis by elevating oxidative stress (21). In light of the aforementioned findings, for the purpose of determining independent risk factors for hepatocellular carcinoma, careful analyses are needed controlling for severity of liver fibrosis, as well as for viral etiologic factors.

With the aim of determining whether HBV or HCV infections, alcohol consumption, smoking, coffee drinking, BMI, and diabetes mellitus are independent risk factors for hepatocellular carcinoma, and how the effects of these factors might change after adjusting for severity of liver fibrosis, we conducted a nested case-control study among the Adult Health Study longitudinal cohort using stored sera. We also evaluated whether viral etiology and increase of BMI exert synergistic effects on the risk for hepatocellular carcinoma.

Materials and Methods

Cohorts. The Atomic Bomb Casualty Commission and its successor, the Radiation Effects Research Foundation, established the Adult Health Study longitudinal cohort in 1958, in which 20,000 age-, gender-, and city-matched proximal and distal atomic bomb survivors and persons not present in the cities at the time of bombings have been examined biennially in outpatient clinics in Hiroshima and Nagasaki.

Study Population. Serum samples obtained from the study participants on each occasion of visiting outpatient clinics have been collected and stored systematically since 1969 (22). Incident cancer cases were identified through the Hiroshima Tumor and Tissue Registry and Nagasaki Cancer Registry, supplemented by additional cases detected via pathologic review of related diseases (23). There were 359 primary hepatocellular carcinoma cases among Adult Health Study participants diagnosed between 1970 and 2002, who visited our outpatient clinics before their diagnosis. Of these, 130 cases were excluded because of nonavailability of stored serum or having only one stored sample. The other 229 cases had serum samples obtained within 6 years before hepatocellular carcinoma diagnosis. After excluding five cases with inadequate stored serum, 224 cases remained for our study. For each case, three controls were selected from the cohort in nested case-control fashion. Nested control selection was random among those who matched the case on gender, age (±2 years), city, time of serum storage (±2 years), and method of serum storage, and countermatched on radiation exposure (24). Although the total number of potential matched control serum samples is 672, because of occasional lack of subjects with stored sera who met the matching and countermatching criteria, the total number of control serum samples actually used was 644.

Laboratory Tests. HBV surface antigen and antibody to hepatitis B core antigen were measured by enzyme immunoassay, and anti-HCV antibody was measured by second-generation enzyme immunoassay as previously described (22, 25). Qualitative detection of HCV RNA among anti-HCV–positive samples was done using a thermocycler (Whatman Biometra) with two sets of PCR primers corresponding to the 5′-untranslated region, as previously described (25). Qualitative detection of HCV RNA was conducted at least twice. HBV infection (HBV+) status was defined as positive for HBV surface antigen or having a high titer of the antibody to hepatitis B core antigen. HCV infection (HCV+) status was defined as positive for HCV RNA (25). Hyaluronic acid and type IV collagen as liver fibrosis markers were measured using an autoanalyzer (Hitachi 7180, Hitachi, Ltd.) and latex agglutination–turbidimetric immunoassay (Fujirebio, Inc., Daiichi Pure Chemicals Co. Ltd.). Ferritin was measured using an autoanalyzer (Hitachi 7180, Hitachi) and colloidal gold immunoassay (Alfresa Pharma Corporation). Platelet count was measured using an automatic blood cell counter at the time of serum storage.

Information on Covariates. Self-administered questionnaires on various lifestyle factors were given to participants in 1965 during attendance at the Adult Health Study examination and in 1978 by mail survey. Information from the 1978 survey was obtained before hepatocellular carcinoma diagnosis for all but 19 (15%) of the cases. Information on alcohol consumption was obtained from the 1965 questionnaire when available, with missing data complemented using the 1978 survey. Alcohol consumption per volume of each type of alcoholic beverage was quantified as previously described (26), and mean ethanol amounts were calculated as grams per day. Information on smoking habits was obtained from the 1965 questionnaire; subjects were divided into the following categories: never, prior, and current smoker. Information on coffee drinking was obtained from the 1978 survey; subjects were divided into the following categories of frequency of coffee consumption: never, 1 day per week, 2 to 4 days per week, and almost daily. Disease diagnoses were based on the International Classification of Diseases (ICD) codes: diabetes mellitus was defined by ICD-7 code 260, ICD-8 code 250, ICD-9 code 250, and ICD-10 codes E10 through E14. BMI (kg/m^2) was calculated from height and weight measured at the Adult Health Study examination.

Subjects were classified based on BMI quintiles with cut points of 19.5, 21.2, 22.9, and 25.0. The number of hepatocellular carcinoma cases with BMI of >30.0 kg/m^2 was too small to be analyzed in detail. Following the recommendations for Asian people by the WHO, the International Association for the Study of Obesity, and the International Obesity Task Force (27), 21.3 to 22.9 kg/m^2 was considered as normal, 23 to 25 kg/m^2 as overweight, and >25.0 kg/m^2 as obese in the present study. We used information on diabetes mellitus and BMI obtained 10 years before the time of hepatocellular

Table 1. Characteristics of hepatocellular carcinoma cases and controls

Study variables	Hepatocellular carcinoma cases (n = 224)			Controls (n = 644)		
	Complete data (%)	n (%)	Mean (SD)	Complete data (%)	n (%)	Mean (SD)
Matched variables						
Gender	100			100		
Male		136 (60.7)			387 (60.1)	
Female		88 (39.3)			257 (39.9)	
Age at hepatocellular carcinoma diagnosis (y)	100		67.6 (10.1)	—		—
City	100			100		
Hiroshima		155 (69.2)			444 (68.9)	
Nagasaki		69 (30.8)			200 (31.1)	
Age at serum storage (y)	100		66.4 (10.2)	100		63.7 (9.8)
Unmatched variables						
Etiology (HBV/HCV status)	94.2			99.4		
HBV−/HCV−		45 (21.3)			579 (90.5)	
HBV+/HCV−		29 (13.7)			18 (2.8)	
HBV−/HCV+		132 (62.6)			41 (6.4)	
HBV+/HCV+		5 (2.4)			2 (0.3)	
Fibrosis markers	94.2			99.4		
Hyaluronic acid (ng/mL)			288.6 (284.6)			69.1 (108.3)
Type IV collagen (ng/mL)			245.2 (136.9)			148.8 (122.1)
Platelet count ($\times 10^4/\mu L$)	67.4		13.0 (6.0)	70.0		22.4 (6.2)
Ferritin (ng/mL)	92.0		250.5 (278.6)	98.6		136.7 (151.0)
Alcohol consumption (g of ethanol per day)	88.8			89.6		
>0 and <20		37 (18.6)			130 (22.5)	
≥20 and <40		20 (10.1)			64 (11.1)	
≥40		45 (22.6)			68 (11.8)	
Current smoking		107 (53.8)			262 (45.3)	
Prior smoking	88.8	12 (6.0)		89.8	33 (5.7)	
Daily coffee drinking	62.1	38 (27.3)		73.3	175 (37.1)	
BMI (kg/m^2) 10 y before diagnosis	93.8			98.3		
≤19.5		38 (18.1)			122 (19.3)	
19.6-21.2		33 (15.7)			136 (21.5)	
21.3-22.9		36 (17.2)			142 (22.4)	
23-25		49 (23.3)			124 (19.6)	
>25		54 (25.7)			109 (17.2)	
Diabetes 10 y before diagnosis	100	18 (8.0)		100	33 (5.1)	
Radiation dose to the liver (Gy)	91.1		0.46 (0.69)	94.1		0.34 (0.56)

carcinoma diagnosis or control matching because these conditions are subject to change because of disease progression in the later stages before diagnosis of hepatocellular carcinoma. Atomic bomb radiation dose was estimated for each subject according to the Dosimetry System DS02 (28).

Ethical Consideration. This nested case-control study was based on RERF Research Protocol 1-04 and approved by the Human Investigation Committee of Radiation Effects Research Foundation.

Statistical Analyses. The nested case-control design is analyzed using a partial likelihood method analogous to that used for cohort follow-up studies (29), which is, in practice, the same as the conditional binary data likelihood for matched case-control studies (30) except that the subjects (cases and controls) in the study are not completely independent because of the possibility of repeated selection. All factors other than radiation were analyzed using relative risks estimated by a log-linear model. The population attributable fraction was estimated for individual factors that increased the risk for hepatocellular carcinoma in the present study. Population attributable fraction was calculated as $pd \times [(mRR - 1) / mRR]$, where mRR is the multivariate adjusted relative risk for the covariates and pd is the proportion of cases exposed to the risk factor. Statistical interaction between viral infection and BMI was tested by adding the product of the two factors to the log-linear model, which tests departure from a multiplicative relationship. Reported P values and confidence limits are based on Wald statistics. Although radiation exposure could have been adjusted by matching on radiation dose as an additional matching factor in the control selection (31), in addition to assessing effects of lifestyle factors and viral hepatitis, another purpose of the present study was to examine effects of radiation exposure after adjustment for possible confounding and interaction by these factors, so matching on radiation, which prevents analysis of radiation risk, was not desirable; rather, we countermatched on radiation (29, 32). Radiation risk was analyzed by using an excess relative risk model as has been done previously (33).

Results

Characteristics of Study Population. Characteristics of the 224 hepatocellular carcinoma cases and 644 comparison subjects are shown in Table 1. The mean age of the cases was 67.6 years, and 61% were men. Cases and controls were comparable with respect to gender, age, city, time of serum storage, and method of serum storage by design. Virological and biochemical assays were done on 211 case and 640 control sera because 13 case samples and 4 control samples had insufficient stored sera for these assays. Hepatocellular carcinoma

case sera evidenced a higher prevalence of HBV or HCV infection status, higher values of fibrosis markers and ferritin, and lower platelet counts compared with control sera. Greater proportions of hepatocellular carcinoma cases had a history of alcohol consumption of ≥40 g of ethanol per day, were current smokers, were obese, had diabetes mellitus, and received high radiation doses compared with the controls. In addition, hepatocellular carcinoma cases were less likely than controls to be daily coffee drinkers. There were no important differences in characteristics such as gender, age at hepatocellular carcinoma diagnosis, city, or BMI between hepatocellular carcinoma cases excluded because of nonavailability of stored serum and those included in this study.

Risk Factors for Hepatocellular Carcinoma Development. Table 2 shows the results of univariate and multivariate analyses using HBV and HCV infection status, alcohol consumption, smoking habit, coffee drinking, BMI, diabetes mellitus, and radiation dose. Strong association was found between hepatocellular carcinoma and hepatitis virus infection, resulting in unadjusted relative risks of 33.7 [95% confidence interval (95% CI), 12.7-89.6] for HBV+/HCV− status and 64.5 (95% CI, 29.1-143) for HBV−/HCV+ status. As expected, the risk for hepatocellular carcinoma for alcohol consumption was significant, with an unadjusted relative risk of 1.34 (95% CI, 1.12-1.60) per 20 g of ethanol per day using continuous alcohol consumption and 2.66 (95% CI, 1.55-4.55) at ≥40 g of ethanol per day using grouped alcohol consumption. Although the grouped results suggest that a simple log-linear model in continuous alcohol consumption may not be adequate, a quadratic term did not significantly improve the model (data not shown). Current smoking was significantly associated with hepatocellular carcinoma risk, with an unadjusted relative risk of 1.87 (95% CI, 1.14-3.07). Daily coffee drinking was associated with decreased risk for hepatocellular carcinoma, with an unadjusted relative risk of 0.51 (95% CI, 0.29-0.90). The presence of obesity and diabetes mellitus 10 years before diagnosis were statistically associated with increased risk for hepatocellular carcinoma, resulting in unadjusted relative risks of 1.88 (95% CI, 1.13-3.13) and 1.88 (95% CI, 1.01-3.50), respectively. The relative risk for a 1-unit difference in BMI was 1.04 (95% CI, 0.99-1.09). Radiation exposure was marginally significantly associated with increased risk for hepatocellular carcinoma ($P = 0.055$).

The risks for viral infection in multivariate analysis did not meaningfully differ from those obtained in the univariate analysis. Alcohol consumption of ≥40 g of ethanol per day and obesity remained significant risk factors for hepatocellular carcinoma even after adjusting for viral infection status and the other factors, whereas the effects of current smoking and diabetes mellitus became nonsignificant after adjustment. Daily coffee drinking was marginally significantly associated with decreased risk for hepatocellular carcinoma after adjustment for viral infection and the other factors. The adjusted relative risk for a one unit difference in BMI, 1.12 (95% CI, 1.03-1.22), was statistically significant, but a quadratic term was not significant.

Table 3 shows the estimated population attributable fraction based on the multivariate adjusted relative risks in the present study. The proportion of hepatocellular

Table 2. Relative risks of hepatocellular carcinoma for individual factors

Variables	Unadjusted		Multivariate adjusted	
	RR (95% CI)	*P*	RR (95% CI)*	*P*
Etiology (HBV/HCV status)				
HBV−/HCV−	1	—	1	—
HBV+/HCV−	33.7 (12.7-89.6)	<0.001	45.8 (15.2-138)	<0.001
HBV−/HCV+	64.5 (29.1-143)	<0.001	101 (38.7-263)	<0.001
HBV+/HCV+	42.4 (6.2-291)	<0.001	70.7 (8.3-601)	<0.001
Alcohol consumption (g of ethanol per day)				
Never	1	—	1	—
>0 and <20	1.11 (0.69-1.78)	>0.5	1.27 (0.56-2.87)	>0.5
≥20 and <40	1.07 (0.57-1.99)	>0.5	1.02 (0.34-3.05)	>0.5
≥40	2.66 (1.55-4.55)	<0.001	4.36 (1.48-13.0)	0.008
Continuous (per 20-g ethanol per day)	1.34 (1.12-1.60)	<0.001	1.73 (1.19-2.52)	0.004
Smoking habit				
Never	1	—	1	—
Current smoking	1.87 (1.14-3.07)	0.014	2.03 (0.82-4.98)	0.13
Prior smoking	1.80 (0.81-3.99)	0.15	1.12 (0.25-5.07)	>0.5
Coffee drinking				
Never	1	—	—	—
Daily	0.51 (0.29-0.90)	0.016	0.40 (0.16-1.02)	0.055
BMI (kg/m^2) 10 y before diagnosis				
≤19.5	1.24 (0.73-2.11)	0.43	1.31 (0.51-3.34)	>0.5
19.6-21.2	0.97 (0.55-1.70)	>0.5	1.24 (0.43-3.54)	>0.5
21.3-22.9	1	—	1	—
23-25	1.61 (0.96-2.70)	0.074	2.51 (0.99-6.37)	0.053
>25	1.88 (1.13-3.13)	0.016	4.57 (1.85-11.3)	<0.001
Continuous (+1 kg/m^2 difference)	1.04 (0.99-1.09)	0.087	1.12 (1.03-1.22)	0.010
Diabetes 10 y before diagnosis	1.88 (1.01-3.50)	0.047	1.98 (0.63-6.27)	0.24

Abbreviation: RR, relative risk.
*Adjusted for hepatitis virus infection, continuous alcohol consumption, smoking habit, coffee drinking, BMI, diabetes mellitus, and radiation dose to the liver.

Table 3. Estimated population attributable fraction of hepatocellular carcinoma for risk factors in this study population

Variables*	Proportion of cases exposed (%)	Multivariate-adjusted RR	Population attributable fraction (%)
Etiology (HBV/HCV status)			
HBV+/HCV−	13.7	45.8	13.4
HBV−/HCV+	62.6	101	62.0
HBV+/HCV+	2.4	70.7	2.4
Alcohol consumption			
≥40-g ethanol per day	22.6	4.36	17.4
BMI 10 y before diagnosis			
>25 kg/m^2	25.7	4.57	20.1

*Population attributable fraction was estimated only for the significant hepatocellular carcinoma risk factors.

carcinoma cases that is attributable to HBV+/HCV−, HBV−/HCV+, HBV+/HCV+, alcohol consumption of ≥40 g of ethanol per day, and obesity were 13.4%, 62.0%, 2.4%, 17.4%, and 20.1%, respectively. These values are not mutually exclusive because some cases were exposed to more than one risk factor.

Analyses with Adjustment for Variables Associated with Severity of Liver Fibrosis. Table 4 shows results for univariate analyses incorporating biomarkers associated with progression of liver fibrosis, such as hyaluronic acid and type IV collagen of fibrosis markers, platelet count, and ferritin. Large statistically significant differences in the mean values of these variables were observed between hepatocellular carcinoma cases and controls. Figure 1 shows a comparison of multivariate analysis results with or without adjustment for ln(type IV collagen) and platelet count using HBV and HCV infection status, alcohol consumption, smoking habit, coffee drinking, BMI, diabetes mellitus, and radiation dose as adjustment variables. We evaluated type IV collagen and platelet count as surrogate markers associated with severity of liver fibrosis. Hepatocellular carcinoma risk for hepatitis virus infection status after adjusting for liver fibrosis meaningfully decreased compared with the results indicated in the previous multivariate analysis, with relative risks of 20.8 (95% CI, 4.8-90.3) and 37.8 (95% CI, 12.4-115) for HBV+/HCV− status and HBV−/HCV+ status, respectively (Fig. 1A). Effects of ≥40 g of ethanol per day and daily coffee drinking decreased and disappeared, respectively, so that adjustment for liver fibrosis decreased the effect of these factors on risk for hepatocellular carcinoma. Current smoking became marginally significantly associated with increased risk for hepatocellular carcinoma after adjusting for liver fibrosis. Obesity remained a significant risk factor independent of adjustment for severity of liver fibrosis, and the relative risk for diabetes mellitus did not meaningfully differ from that without such adjustment (Fig. 1B).

Interaction between Hepatitis Virus Infection Status and Increase of BMI. Table 5 shows the joint effects of hepatitis virus infection status and BMI, with adjustment for alcohol consumption, smoking habit, coffee drinking, diabetes mellitus, and radiation dose. Although being obese was clearly a risk factor for hepatocellular carcinoma subjects with adjustment for viral factors, it was not a significant risk factor in those with HBV−/HCV− status. However, despite the appearance of a trend with BMI, only 15 hepatocellular carcinoma cases were identified among HBV−/HCV− individuals with obesity. Among hepatocellular carcinoma subjects with HBV−/HCV+ status, the relative risk increased dramatically with increasing BMI. Linear (P = 0.003) and quadratic (P = 0.013) terms in continuous BMI were

Table 4. Relative risks of hepatocellular carcinoma for variables associated with severity of liver fibrosis: unadjusted relative risk and 95% CI

Variables	Hepatocellular carcinoma cases/controls	Unadjusted	
		RR (95% CI)	P
Liver fibrosis markers	211/640		
Hyaluronic acid (+per 10 ng/mL)		1.10 (1.08-1.12)	<0.001
ln(hyaluronic acid) (+per 1 unit)		5.43 (4.04-7.30)	<0.001
Type IV collagen (+per 10 ng/mL)		1.14 (1.10-1.17)	<0.001
ln(type IV collagen) (+per 1 unit)		80.9 (35.8-183)	<0.001
Platelet count	151/448		
+Per 10^4/μL		0.75 (0.71-0.80)	<0.001
≥25.0 (×10^4/μL)	4/133	1	
20.0-24.9 (×10^4/μL)	19/163	4.5 (1.3-1.6)	0.02
15.0-19.9 (×10^4/μL)	26/105	11.8 (3.2-43)	<0.001
10.0-14.9 (×10^4/μL)	52/42	61 (16-232)	<0.001
<10.0 (×10^4/μL)	50/5	822 (125-5400)	<0.001
Ferritin	206/635		
+ Per 10 ng/mL		1.03 (1.02-1.04)	<0.001
ln(ferritin) (+per 1 unit)		1.51 (1.25-1.82)	<0.001

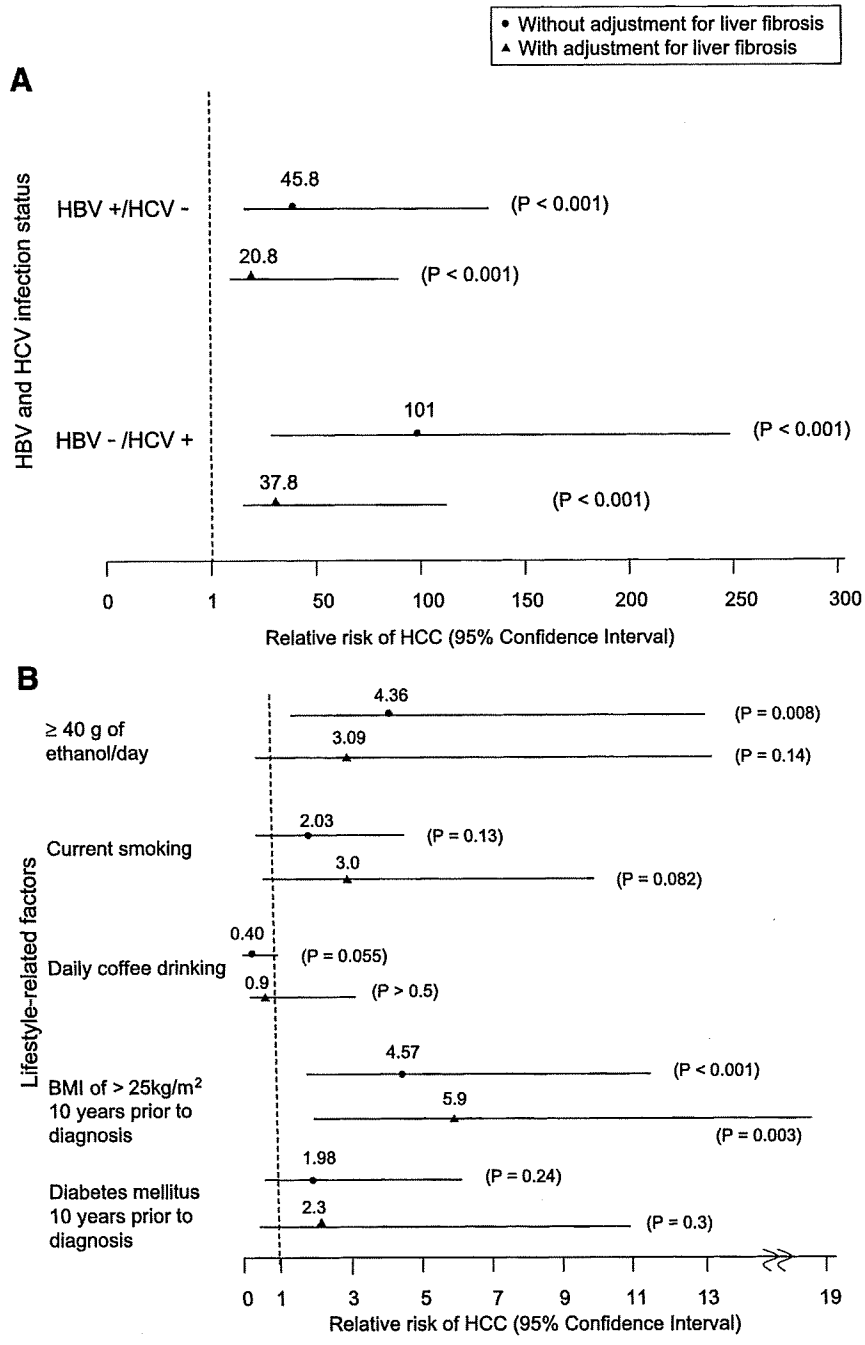

Figure 1. Multivariate relative risk for hepatocellular carcinoma for individual risk factors, with and without adjustment for variables associated with severity of liver fibrosis. Each relative risk was analyzed with and without adjustment for ln(type IV collagen) and platelet count, using HBV and HCV infection status, continuous alcohol consumption, smoking habit, coffee drinking, BMI, diabetes mellitus, and radiation dose as adjustment variables. **A.** HBV and HCV infection status. **B.** Lifestyle-related factors. *HCC,* hepatocellular carcinoma.

significant among HBV−/HCV+ individuals. Among hepatocellular carcinoma subjects with HBV+/HCV− status, the relative risk for hepatocellular carcinoma did not show evidence of an increase with increased BMI, although the examination of a joint effect of HBV infection and BMI was based on only one hepatocellular carcinoma case out of three subjects who were HBV+/HCV− and obese. The reason for the relatively small unadjusted relative risk for obesity (Table 2) might have been due to the small number of cases and controls with HBV+/HCV− status, which apparently offset the increase observed in HBV−/HCV+ status individuals.

Discussion

This nested case-control study indicated that HBV and HCV infection, alcohol consumption of ≥40 g of ethanol per day, and obesity 10 years before hepatocellular carcinoma diagnosis were independent risk factors for hepatocellular carcinoma, and that obesity as well as hepatitis virus infection remained independent risk factors for hepatocellular carcinoma after taking into account the severity of liver fibrosis. Furthermore, significant multiplicative interaction in hepatocellular carcinoma risk between viral etiology and increased BMI was observed in HCV-infected individuals. The